

Searching for dark matter and astrophysical sources with gamma-ray anisotropies

Jennifer Siegal-Gaskins
Caltech

with

A. Cuoco, [T. Linden](#), M.N. Mazziotta, and V. Vitale
on behalf of
the Fermi LAT Collaboration
and E. Komatsu

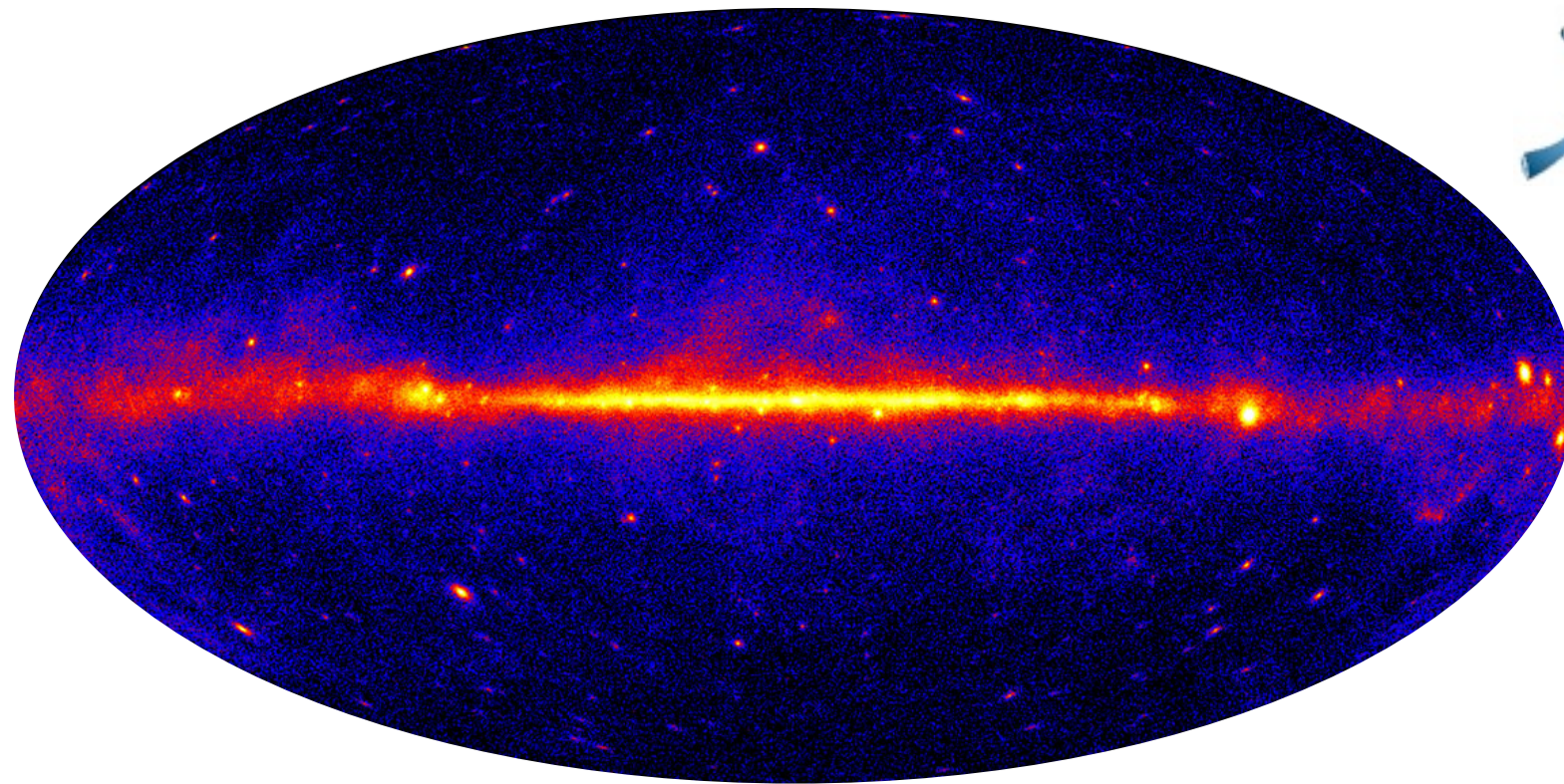
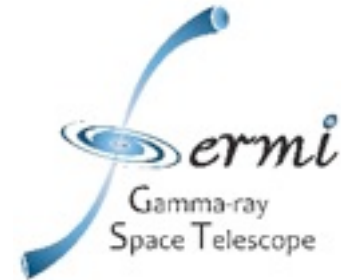
[R. Reesman](#), V. Pavlidou, S. Profumo, and T. Walker
The MultiDark Collaboration

based on

The Fermi LAT Collaboration & Komatsu, arXiv:
1202.2856; accepted to PRD

JSG, Reesman, Pavlidou, Profumo, & Walker, MNRAS 415,
1074S (2011), arXiv:1011.5501

Cuoco, Komatsu, and JSG, arXiv:1202.5309



Jennifer Siegal-Gaskins

Caltech

with

A. Cuoco, [T. Linden](#), M.N. Mazziotta, and V. Vitale
on behalf of
the Fermi LAT Collaboration
and E. Komatsu

based on

The Fermi LAT Collaboration & Komatsu, arXiv:
[1202.2856](#); accepted to PRD

JSG, Reesman, Pavlidou, Profumo, & Walker, MNRAS 415,
1074S (2011), arXiv:[1011.5501](#)

[R. Reesman](#), V. Pavlidou, S. Profumo, and T. Walker
The MultiDark Collaboration

Cuoco, Komatsu, and JSG, arXiv:[1202.5309](#)



Jennifer Siegal-Gaskins

Caltech

with

A. Cuoco, [T. Linden](#), M.N. Mazziotta, and V. Vitale
on behalf of
the Fermi LAT Collaboration
and E. Komatsu

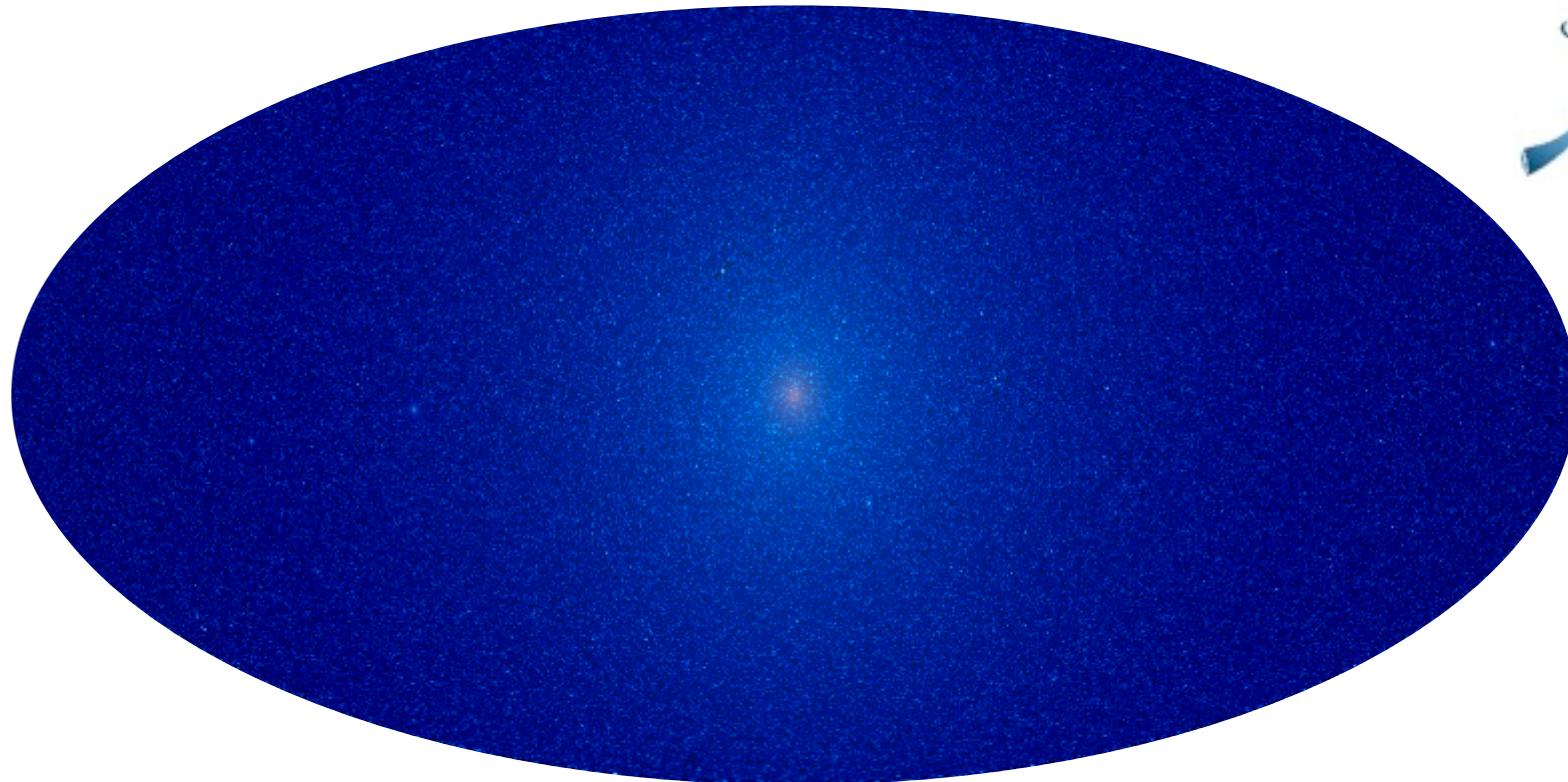
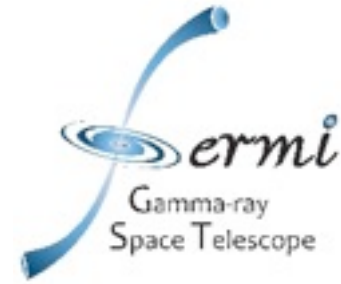
[R. Reesman](#), V. Pavlidou, S. Profumo, and T. Walker
The MultiDark Collaboration

based on

The Fermi LAT Collaboration & Komatsu, arXiv:
1202.2856; accepted to PRD

JSG, Reesman, Pavlidou, Profumo, & Walker, MNRAS 415,
1074S (2011), arXiv:1011.5501

Cuoco, Komatsu, and JSG, arXiv:1202.5309



Jennifer Siegal-Gaskins

Caltech

with

A. Cuoco, [T. Linden](#), M.N. Mazziotta, and V. Vitale
on behalf of
the Fermi LAT Collaboration
and E. Komatsu

[R. Reesman](#), V. Pavlidou, S. Profumo, and T. Walker
The MultiDark Collaboration

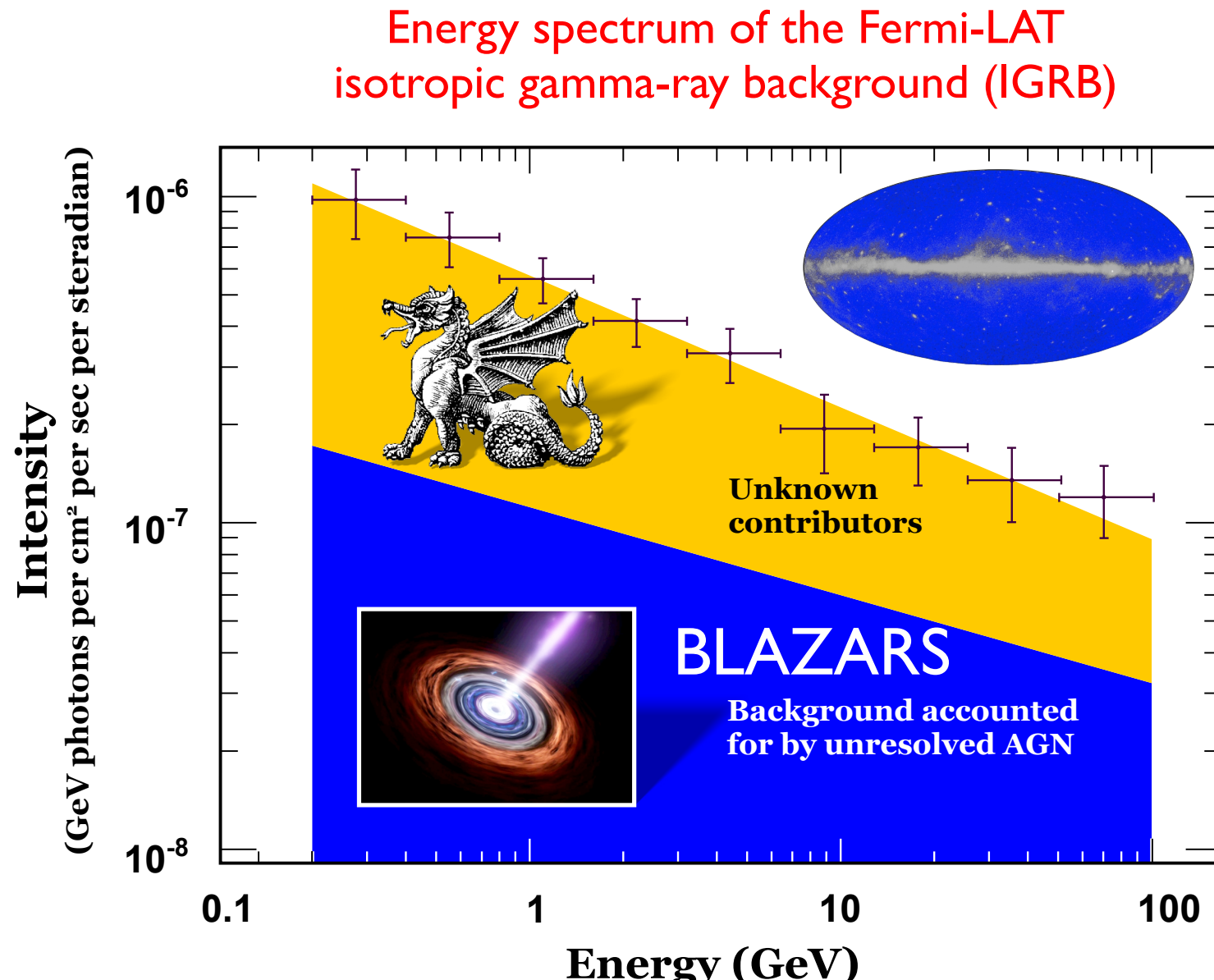
based on

The Fermi LAT Collaboration & Komatsu, arXiv:
1202.2856; accepted to PRD

JSG, Reesman, Pavlidou, Profumo, & Walker, MNRAS 415,
1074S (2011), arXiv:1011.5501

Cuoco, Komatsu, and JSG, arXiv:1202.5309

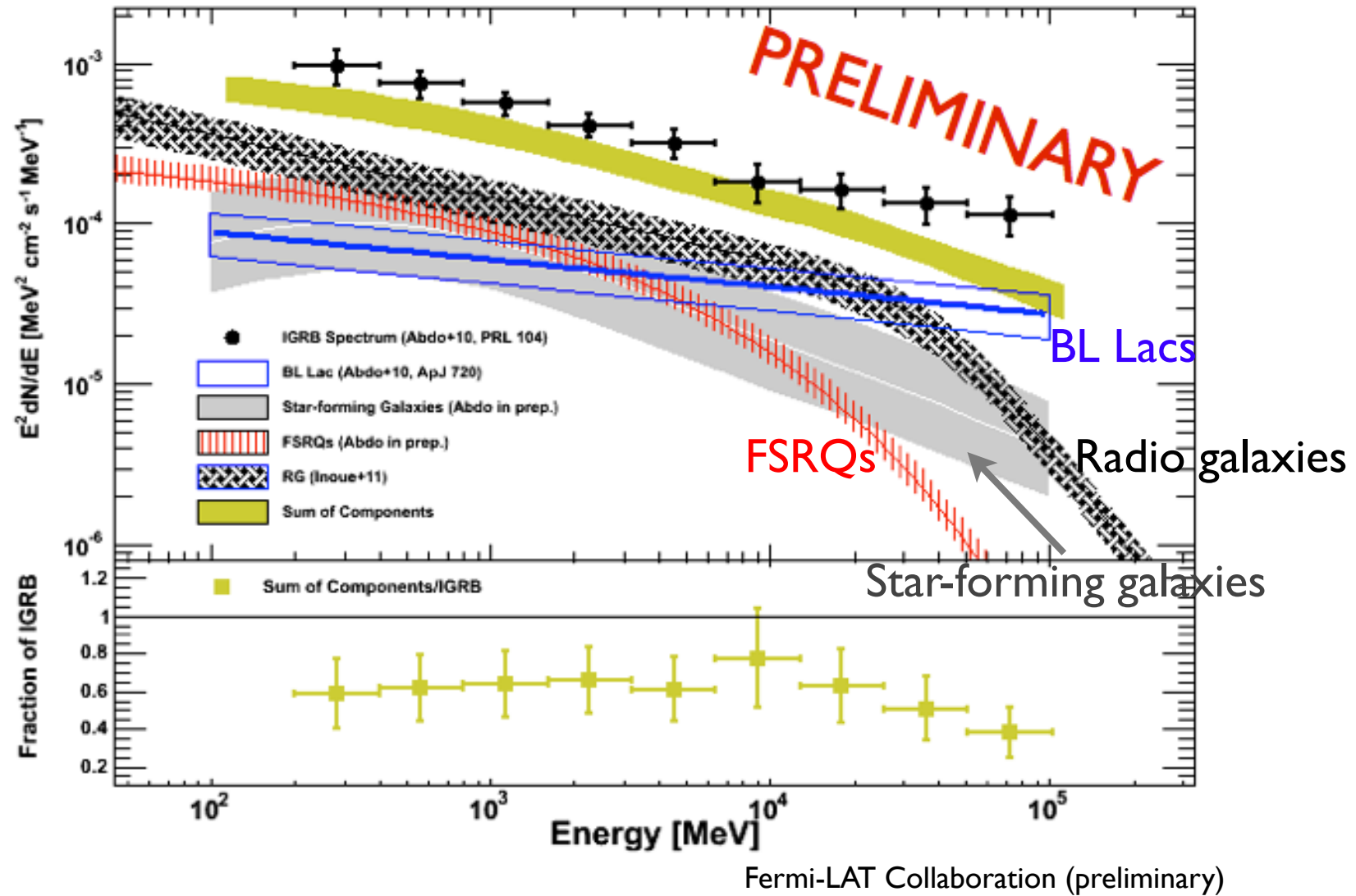
What is making the diffuse gamma-ray background?



Credit: NASA/DOE/Fermi LAT Collaboration

What is making the diffuse gamma-ray background?

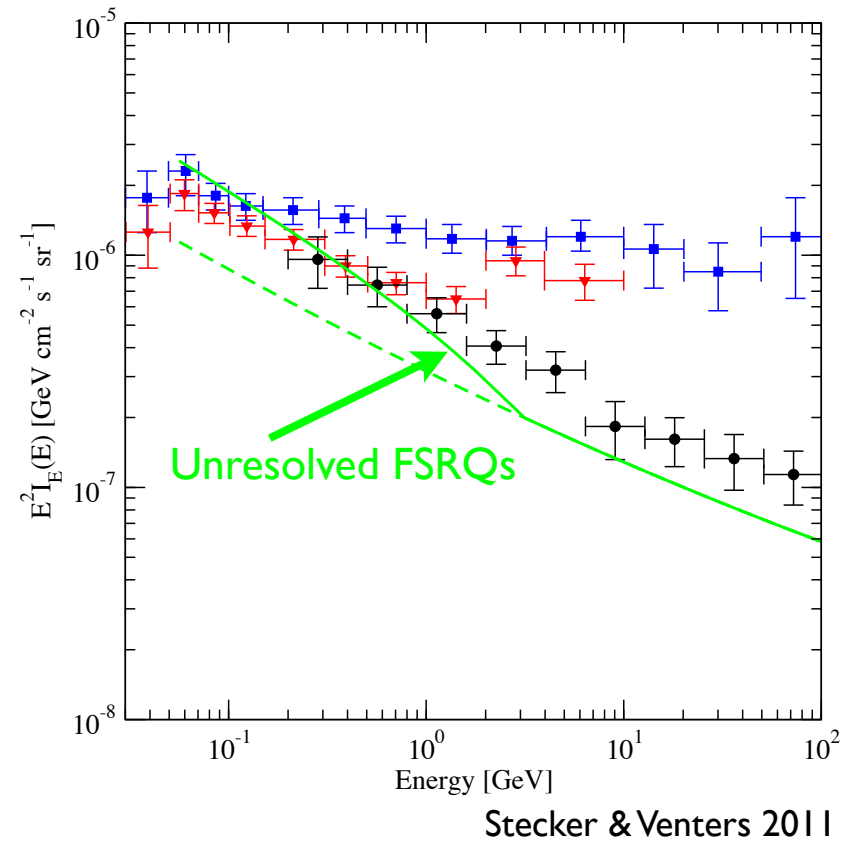
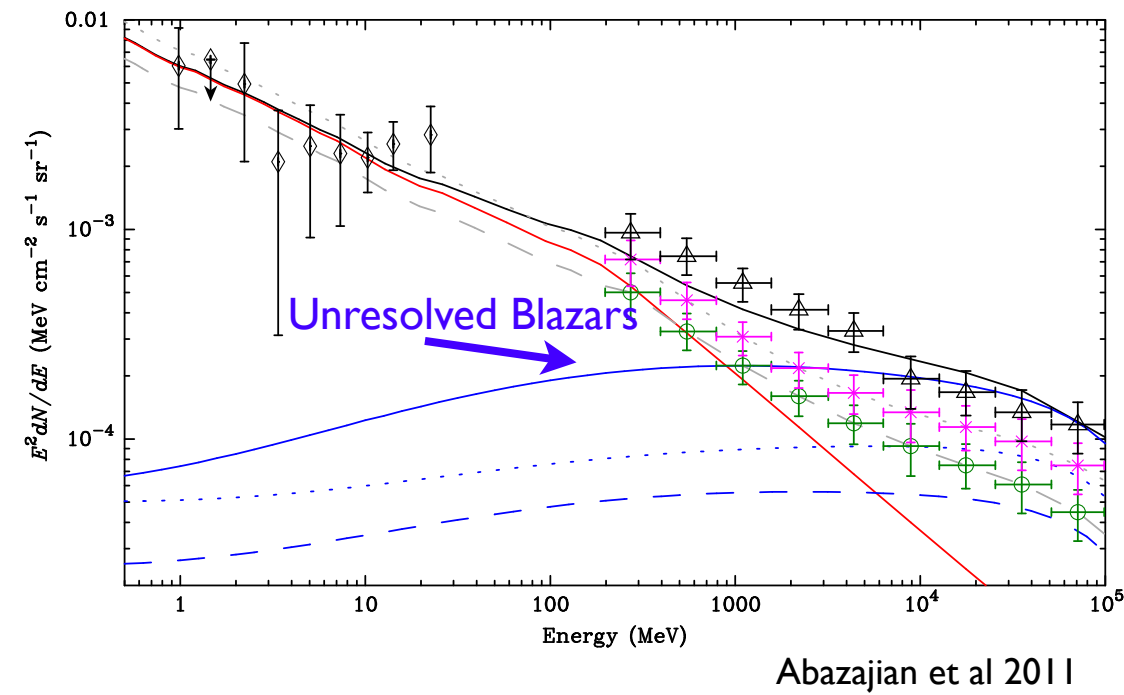
Expected contribution of source populations to the IGRB



Sum is $\sim 40\text{-}70\%$ of IGRB intensity (energy-dependent)

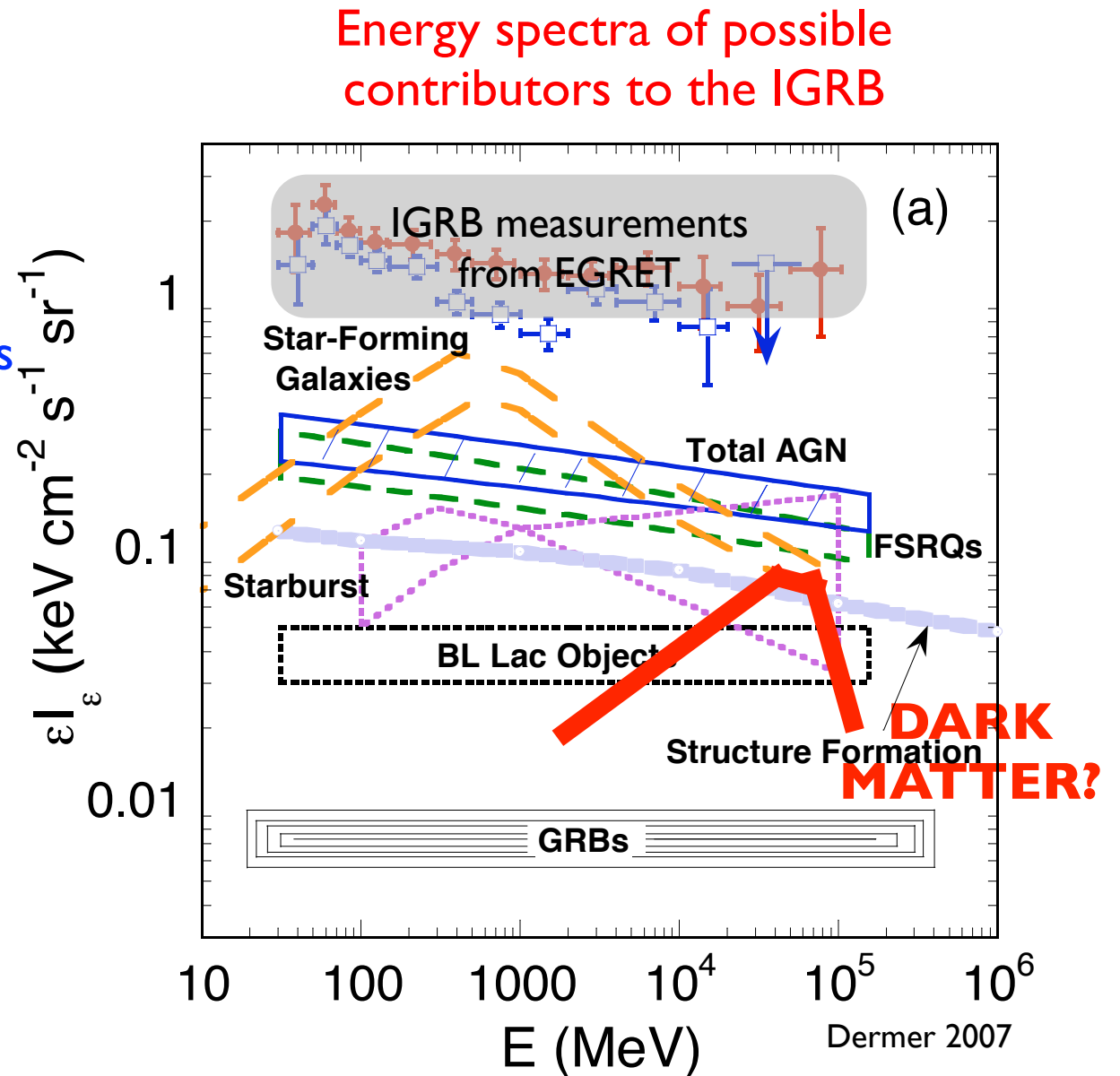
What is making the diffuse gamma-ray background?

Other predictions for the blazar contribution to the IGRB



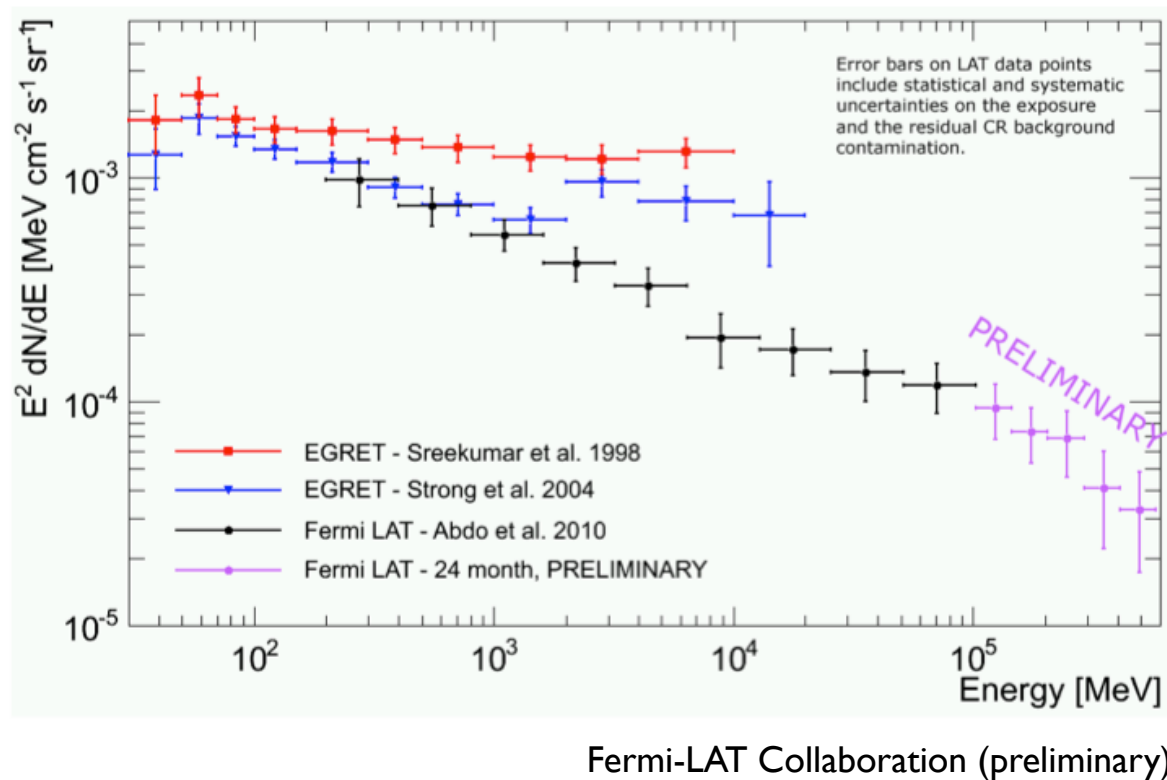
Adding up diffuse GeV emission

- guaranteed contributors include:
 - blazars (but no consensus on size of contribution!)
 - star-forming galaxies
 - millisecond pulsars
- possible contributions from unknown/unconfirmed source classes:
 - dark matter
 - ???

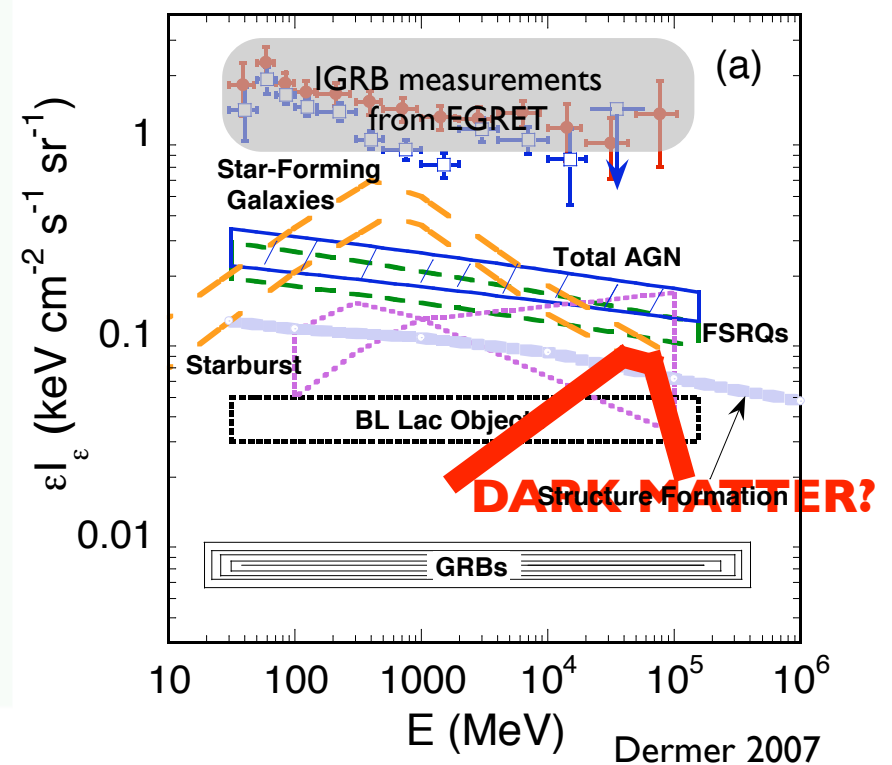


Adding up diffuse GeV emission

Energy spectrum of the Fermi-LAT IGRB



Energy spectra of possible contributors to the IGRB



Relatively featureless total IGRB intensity spectrum → lack of spectral handles to ID individual components!

Detecting unresolved sources with anisotropies



- diffuse emission that originates from one or more **unresolved source populations** will contain **fluctuations on small angular scales** due to variations in the number density of sources in different sky directions
- **the amplitude and energy dependence of the anisotropy** can reveal the presence of multiple source populations and constrain their properties

Detecting unresolved sources with anisotropies



- diffuse emission that originates from one or more **unresolved source populations** will contain **fluctuations on small angular scales** due to variations in the number density of sources in different sky directions
- **the amplitude and energy dependence of the anisotropy** can reveal the presence of multiple source populations and constrain their properties

Anisotropy is another IGRB observable!!!

The angular power spectrum

$$I(\psi) = \sum_{\ell,m} a_{\ell m} Y_{\ell m}(\psi) \quad C_\ell = \langle |a_{\ell m}|^2 \rangle$$

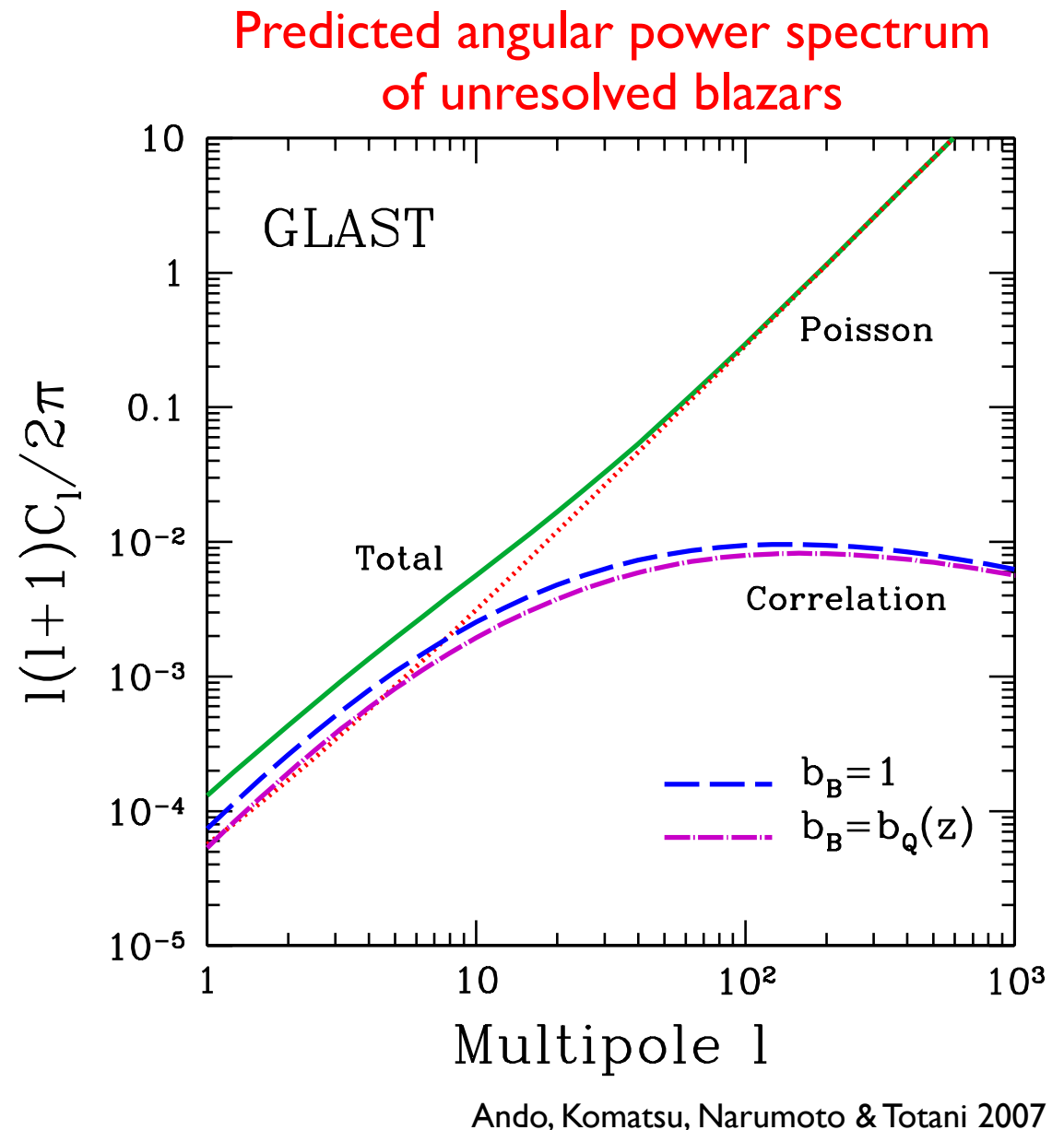
- intensity angular power spectrum: C_ℓ
 - indicates *dimensionful* amplitude of anisotropy
- fluctuation angular power spectrum: $\frac{C_\ell}{\langle I \rangle^2}$
 - *dimensionless*, independent of intensity normalization
 - amplitude for a single source class is the same in all energy bins (if all members have same energy spectrum)

Angular power spectra of unresolved gamma-ray sources

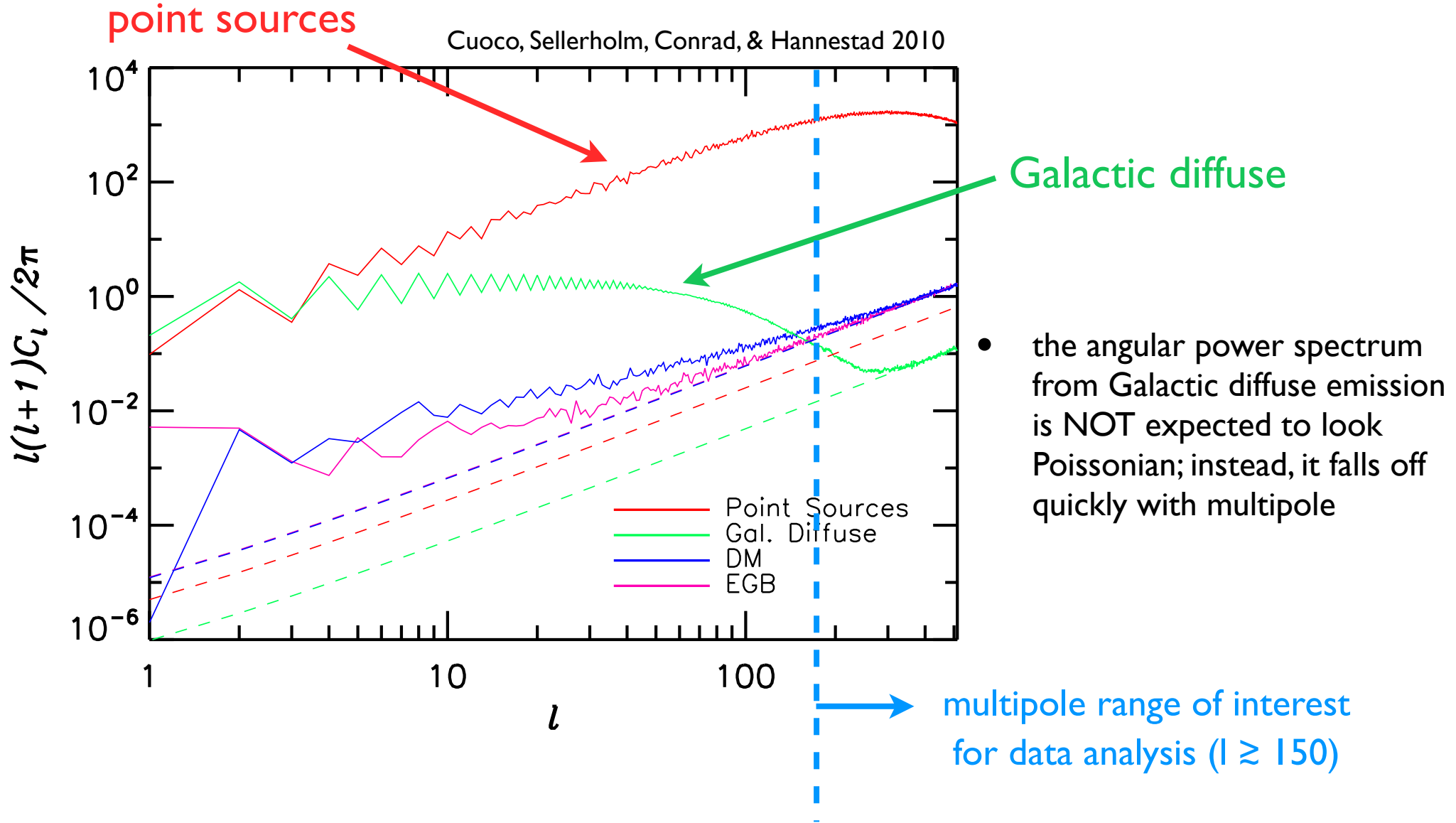
- the angular power spectrum of many gamma-ray source classes (except dark matter) is dominated by the Poisson (shot noise) component for multipoles greater than ~ 10
- Poisson angular power arises from unclustered point sources and takes the same value at all multipoles

predicted fluctuation angular power $C_\ell/\langle I \rangle^2 [\text{sr}]$ at $\ell = 100$ for a single source class
(LARGE UNCERTAINTIES):

- blazars: $\sim 2\text{e-}4$
- starforming galaxies: $\sim 2\text{e-}7$
- dark matter: $\sim 1\text{e-}6$ to $\sim 1\text{e-}4$
- MSPs: ~ 0.03



Angular power spectra of foregrounds



The Fermi Large Area Telescope (*Fermi* LAT)

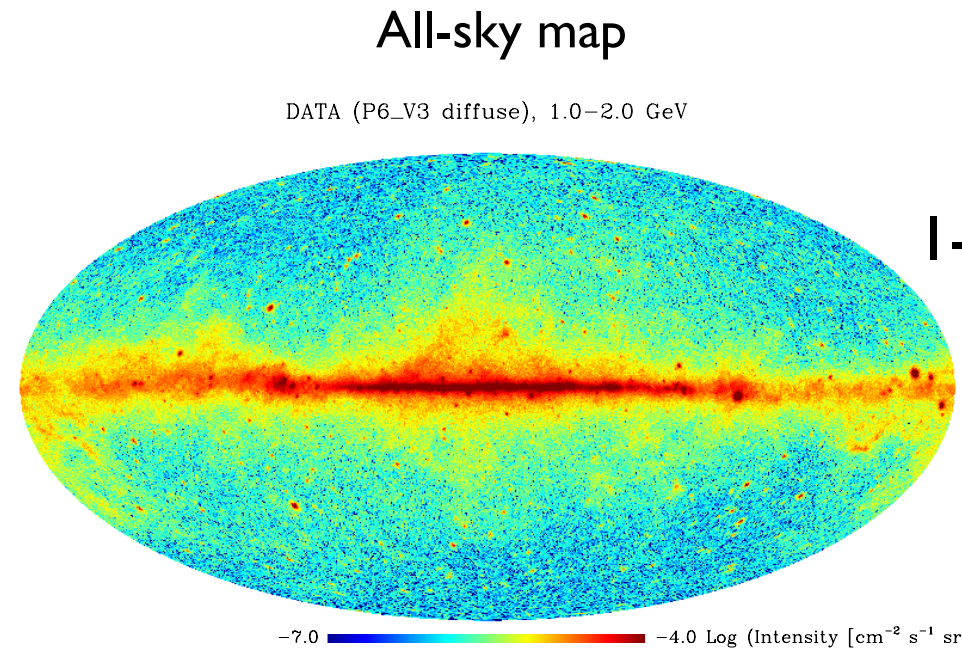
- 20 MeV to > 300 GeV
- Angular resolution ~ 0.1 deg above 10 GeV
- Uniform sky exposure of ~ 30 mins every 3 hrs
- Excellent charged particle background rejection



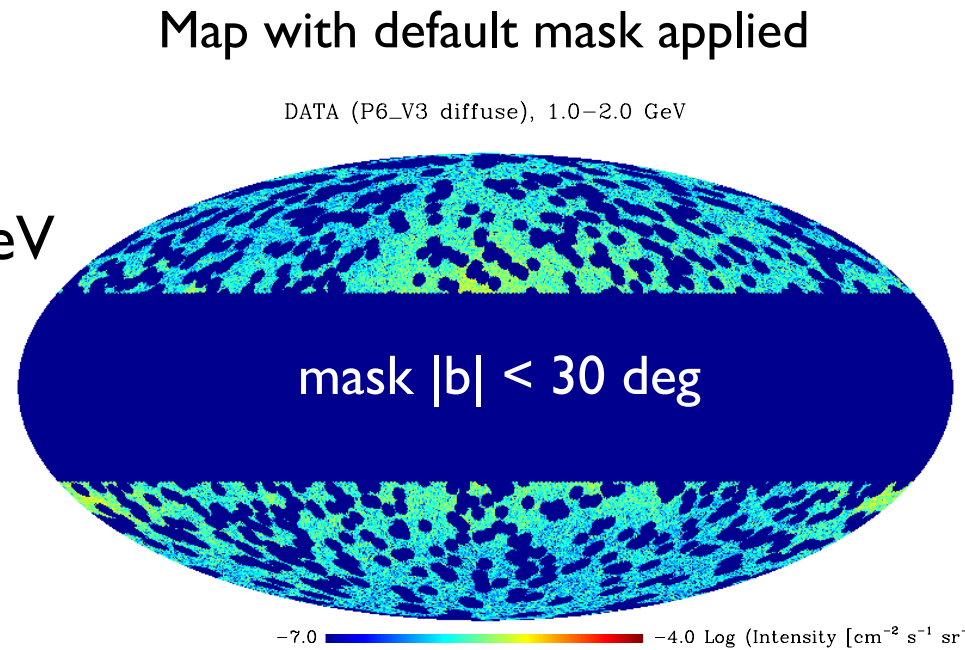
Credit: NASA/General Dynamics



Angular power spectrum analysis of Fermi LAT data

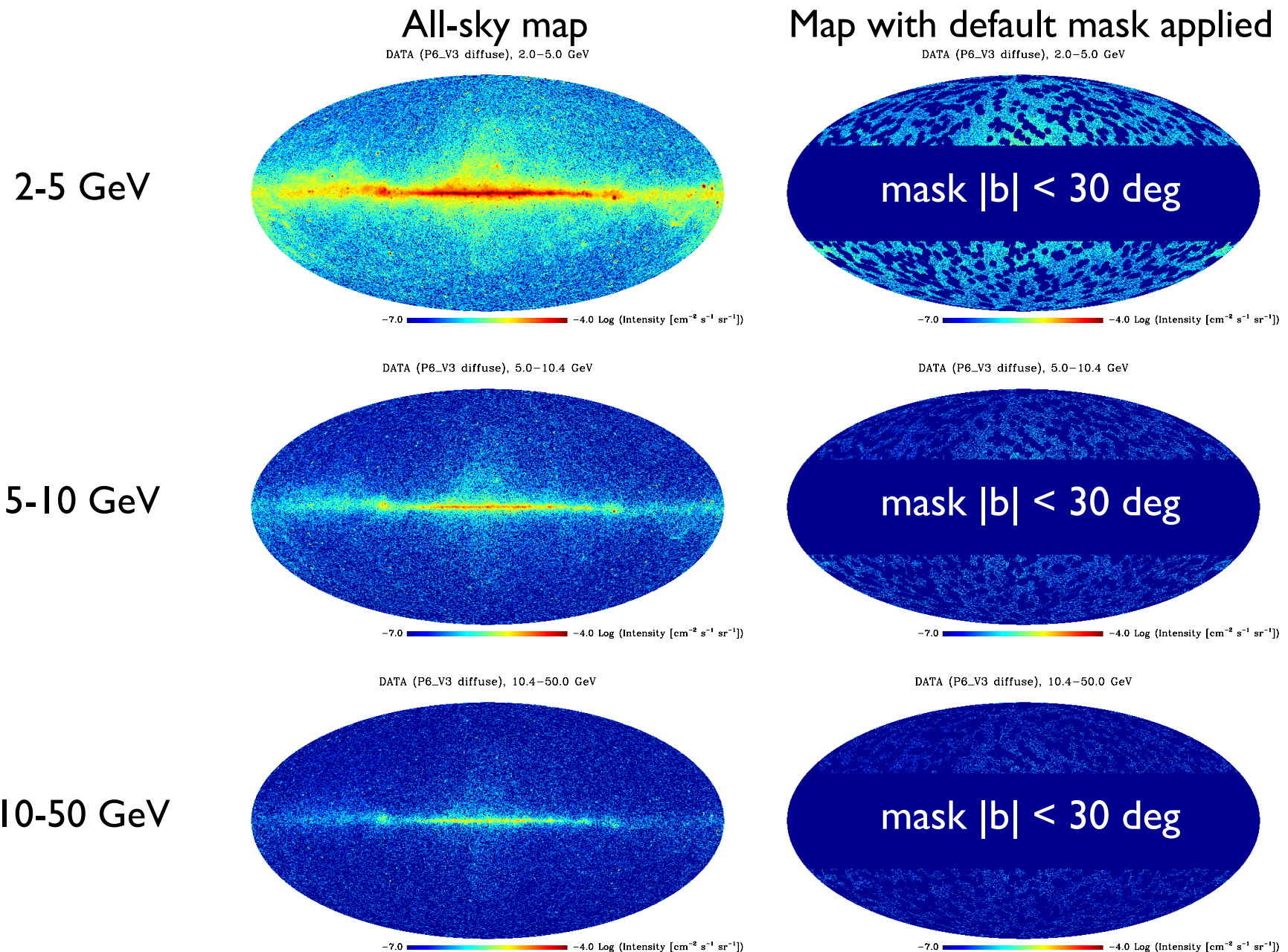


1-2 GeV



- **data selection:** ~ 22 months of data, diffuse class events
- **energy range:** 1 GeV - 50 GeV, divided into 4 energy bins for angular power spectrum analysis
- **masking:** 11-month catalog sources are masked within a 2 deg angular radius, and $|b| < 30$ deg masked to reduce contamination by Galactic diffuse emission

Angular power spectrum analysis of Fermi LAT data



Angular power spectrum analysis of Fermi LAT data

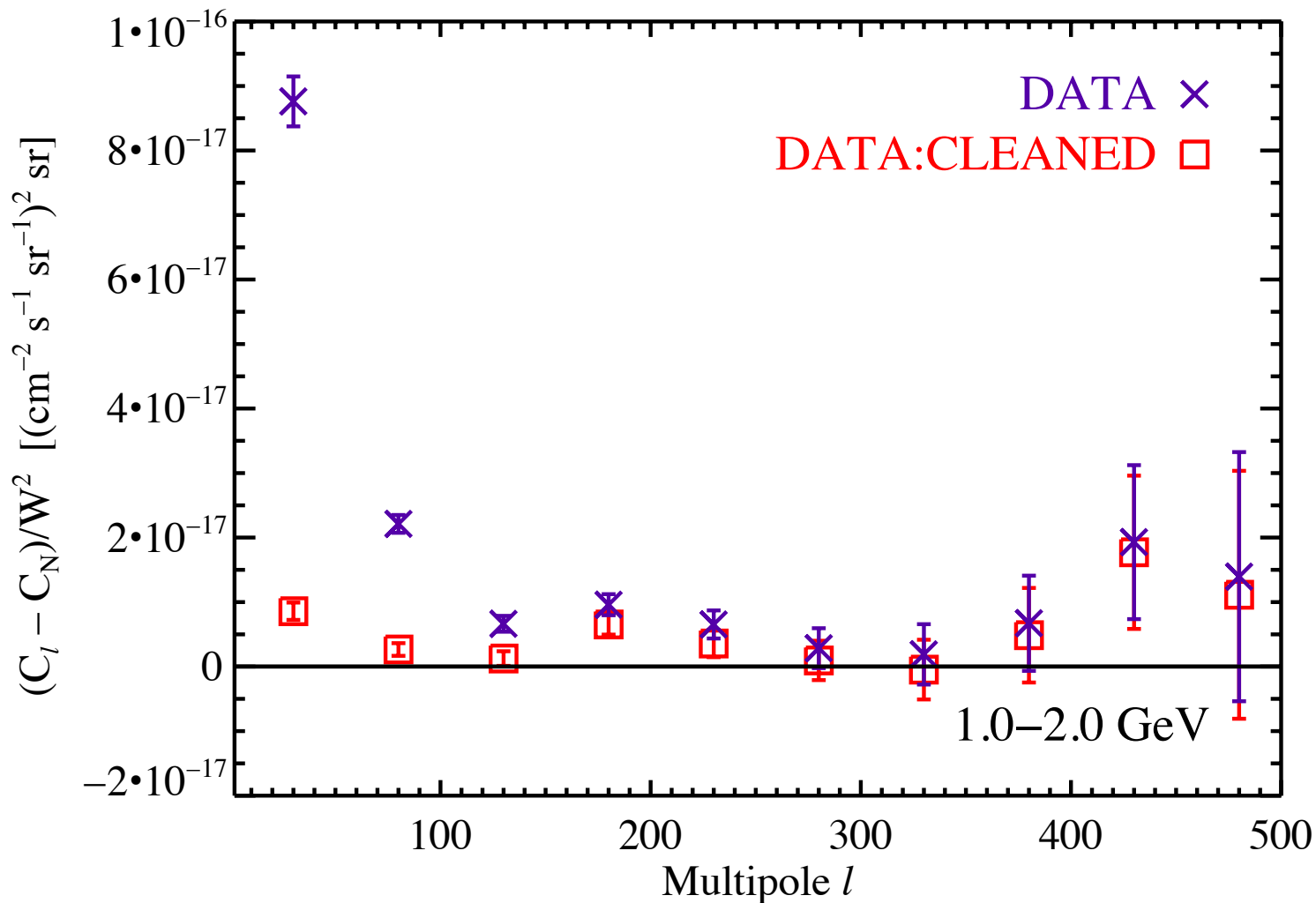
- angular power spectrum calculation: performed using HEALPix (Gorski et al. 2005)
- signal angular power spectrum estimator:

$$C_\ell^{\text{signal}} = \frac{C_\ell^{\text{raw}} / f_{\text{sky}} - C_N}{(W_\ell^{\text{beam}})^2}$$

- corrected for effects of masking (valid above $\ell \sim 10$)
- photon noise is subtracted
- corrected for effects of the PSF (“beam window function”)
- measurement uncertainties: indicate 1-sigma statistical uncertainty, systematic uncertainty not included

Angular power spectra of the data

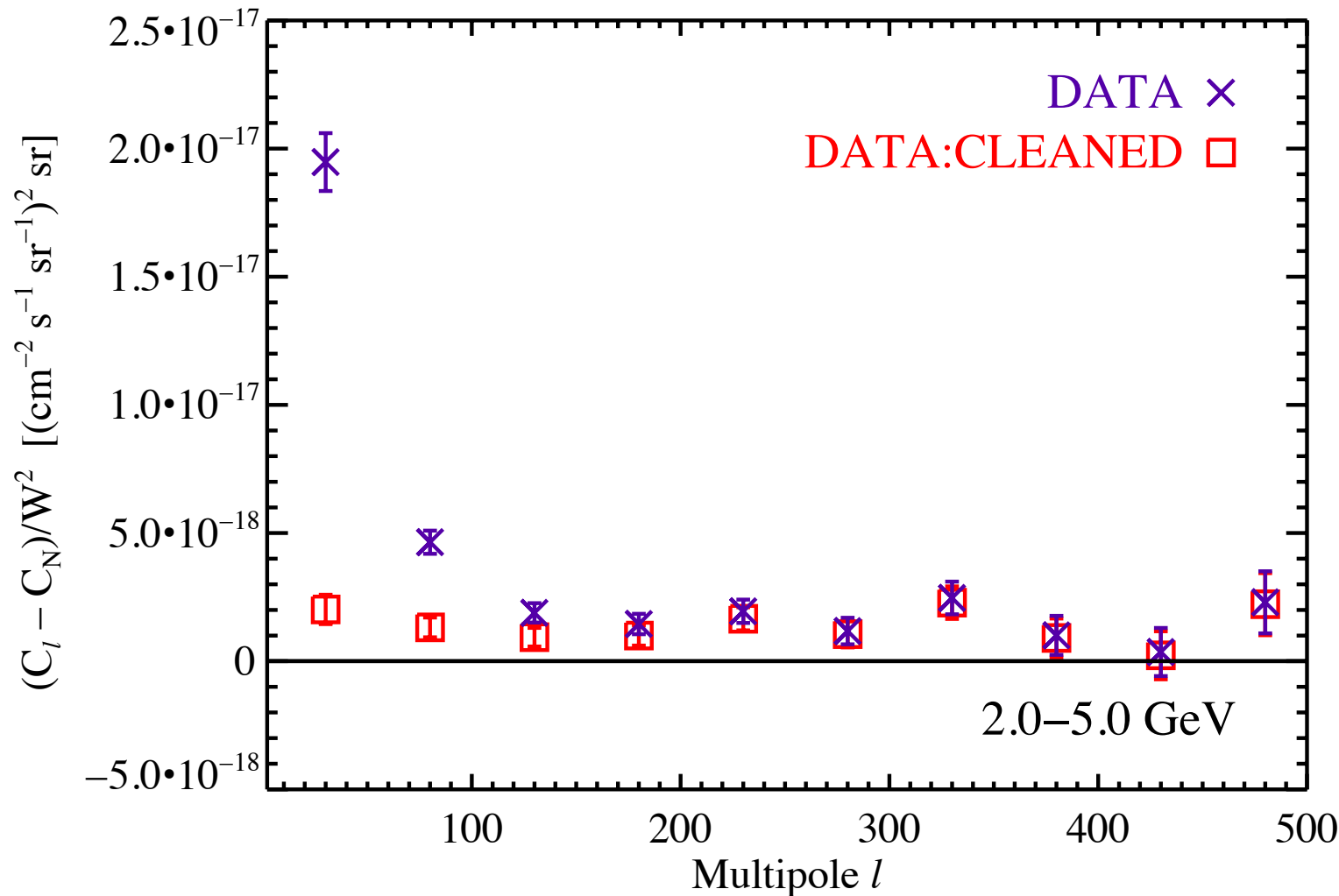
intensity angular power spectra



DATA:CLEANED = DATA - Galactic diffuse model

Angular power spectra of the data

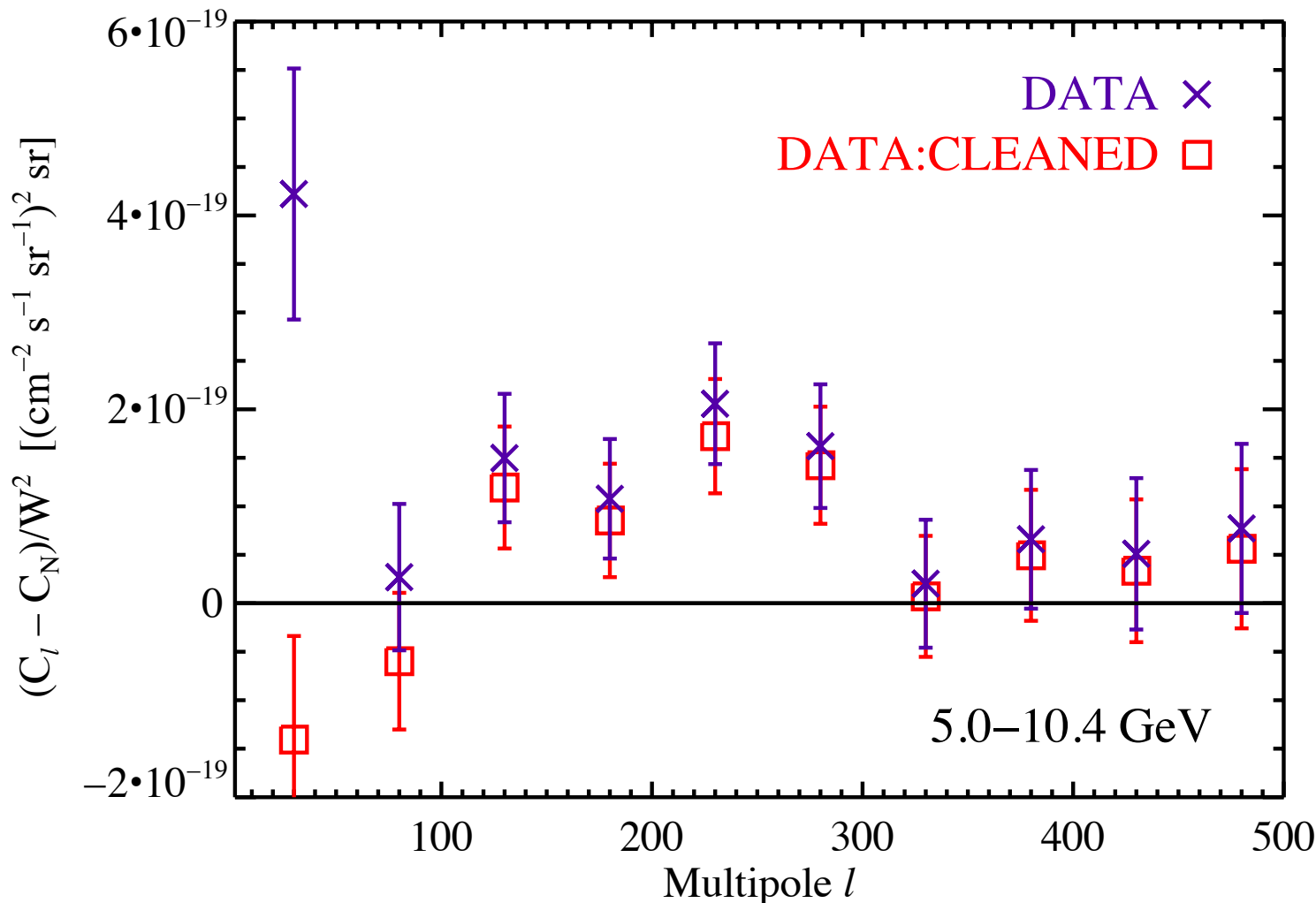
intensity angular power spectra



DATA:CLEANED = DATA - Galactic diffuse model

Angular power spectra of the data

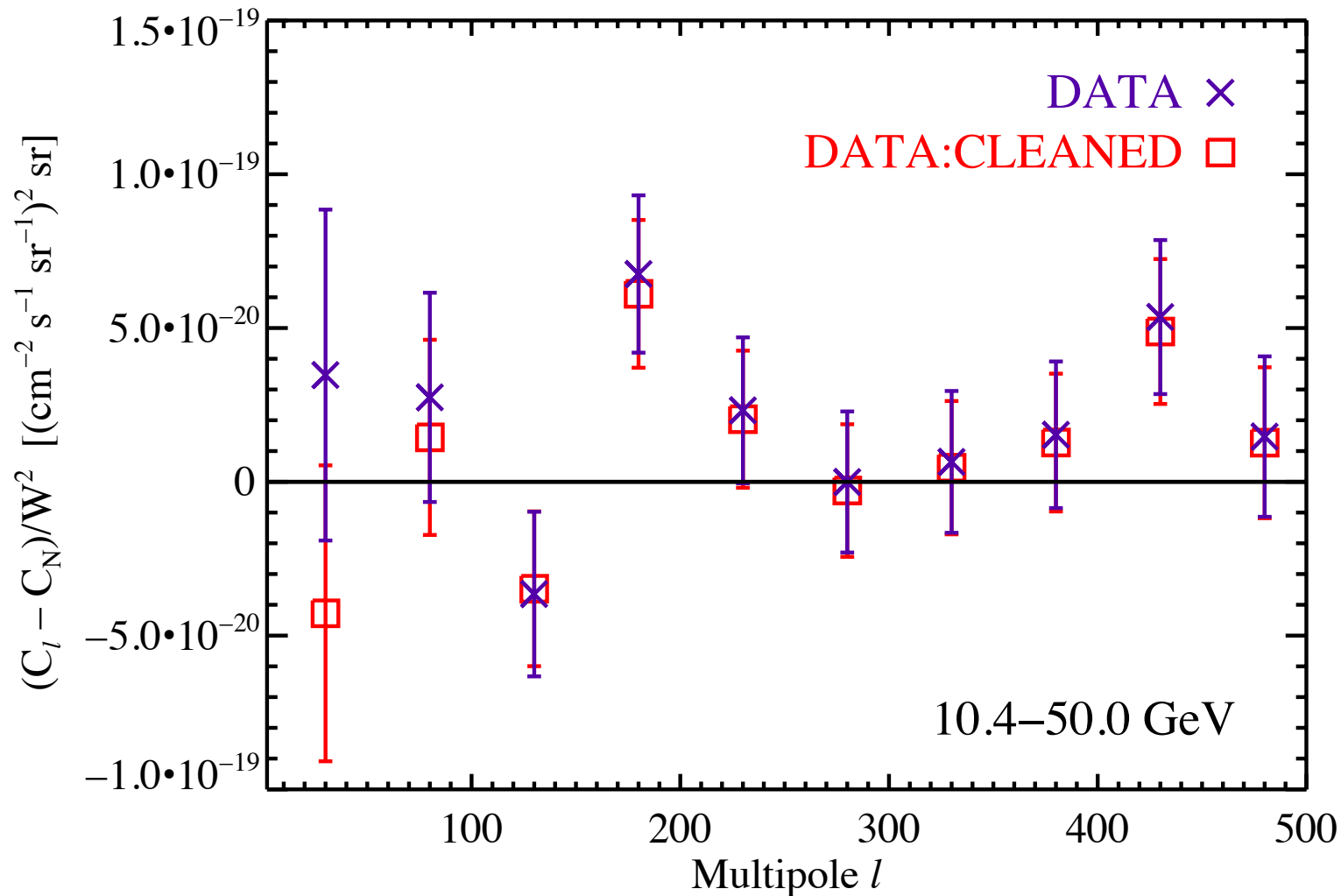
intensity angular power spectra



DATA:CLEANED = DATA - Galactic diffuse model

Angular power spectra of the data

intensity angular power spectra



DATA:CLEANED = DATA - Galactic diffuse model

Angular power in the data

- identifying the signal at $155 \leq l \leq 504$ as Poisson angular power C_P , best-fit value of C_P is determined
- significant ($>3\sigma$) detection of angular power up to 10 GeV, lower significance power measured at 10-50 GeV

E_{min} [GeV]	E_{max} [GeV]	C_P [($\text{cm}^{-2} \text{s}^{-1} \text{sr}^{-1}$) 2 sr]	Significance	$C_P / \langle I \rangle^2$ [10^{-6} sr]
1.04	1.99	$7.39 \pm 1.14 \times 10^{-18}$	6.5σ	10.2 ± 1.6
1.99	5.00	$1.57 \pm 0.22 \times 10^{-18}$	7.2σ	8.35 ± 1.17
5.00	10.4	$1.06 \pm 0.26 \times 10^{-19}$	4.1σ	9.83 ± 2.42
10.4	50.0	$2.44 \pm 0.92 \times 10^{-20}$	2.7σ	8.00 ± 3.37

Comparison with simulated models

- **comparison with simulated all-sky models:** two simulated models of the gamma-ray sky are analyzed; little or no angular power above $\ell \sim 100$ is found, in contrast to the results from the data

	E_{\min} [GeV]	E_{\max} [GeV]	C_P [(cm $^{-2}$ s $^{-1}$ sr $^{-1}$) 2 sr]	Significance	$C_P/\langle I \rangle^2$ [10 $^{-6}$ sr]
MODEL	1.04	1.99	$1.89 \pm 1.08 \times 10^{-18}$	1.7σ	2.53 ± 1.47
	1.99	5.00	$1.92 \pm 2.10 \times 10^{-19}$	0.9σ	0.99 ± 1.12
	5.00	10.4	$3.41 \pm 2.60 \times 10^{-20}$	1.3σ	3.04 ± 2.34
	10.4	50.0	$0.62 \pm 9.63 \times 10^{-21}$	0.1σ	0.24 ± 3.02

Significance of difference in angular power
between data and model

E_{\min}	E_{\max}	Significance of ΔC_P
1.04	1.99	3.5σ
1.99	5.00	4.5σ
5.00	10.4	2.0σ
10.4	50.0	1.7σ

Comparison with predicted angular power

Fluctuation angular power in data

$C_P / \langle I \rangle^2$ [10^{-6} sr]
10.2 ± 1.6
8.35 ± 1.17
9.83 ± 2.42
8.00 ± 3.37

predicted fluctuation angular power $C_\ell / \langle I \rangle^2$ [sr] at $\ell = 100$ for a single source class
(LARGE UNCERTAINTIES):

- blazars: $\sim 2\text{e-}4$
- starforming galaxies: $\sim 2\text{e-}7$
- dark matter: $\sim 1\text{e-}6$ to $\sim 1\text{e-}4$
- MSPs: ~ 0.03

- fluctuation angular power of $\sim 1\text{e-}5$ sr falls in the range predicted for some astrophysical source classes and some dark matter scenarios
- can be used to constrain the IGRB contribution from these populations

Source population constraints from anisotropy

- intensity angular power can constrain the absolute IGRB contribution from a single population

$$C_{P,i} \leq C_{P,\text{tot}}$$

- fluctuation angular power can constrain the fractional IGRB contribution from a single population

$$f_i^2 \leq \frac{C_{P,\text{tot}} / \langle I_{\text{tot}} \rangle^2}{C_{P,i} / \langle I_i \rangle^2}$$

Constraints from the fluctuation angular power

Constraints from best-fit constant fluctuation angular power ($\ell \geq 150$)
measured in the data and foreground-cleaned data

Source class	Predicted $C_{100}/\langle I \rangle^2$ [sr]	Maximum fraction of IGRB intensity	
		DATA	DATA:CLEANED
Blazars	2×10^{-4}	21%	19%
Star-forming galaxies	2×10^{-7}	100%	100%
Extragalactic dark matter annihilation	1×10^{-5}	95%	83%
Galactic dark matter annihilation	5×10^{-5}	43%	37%
Millisecond pulsars	3×10^{-2}	1.7%	1.5%

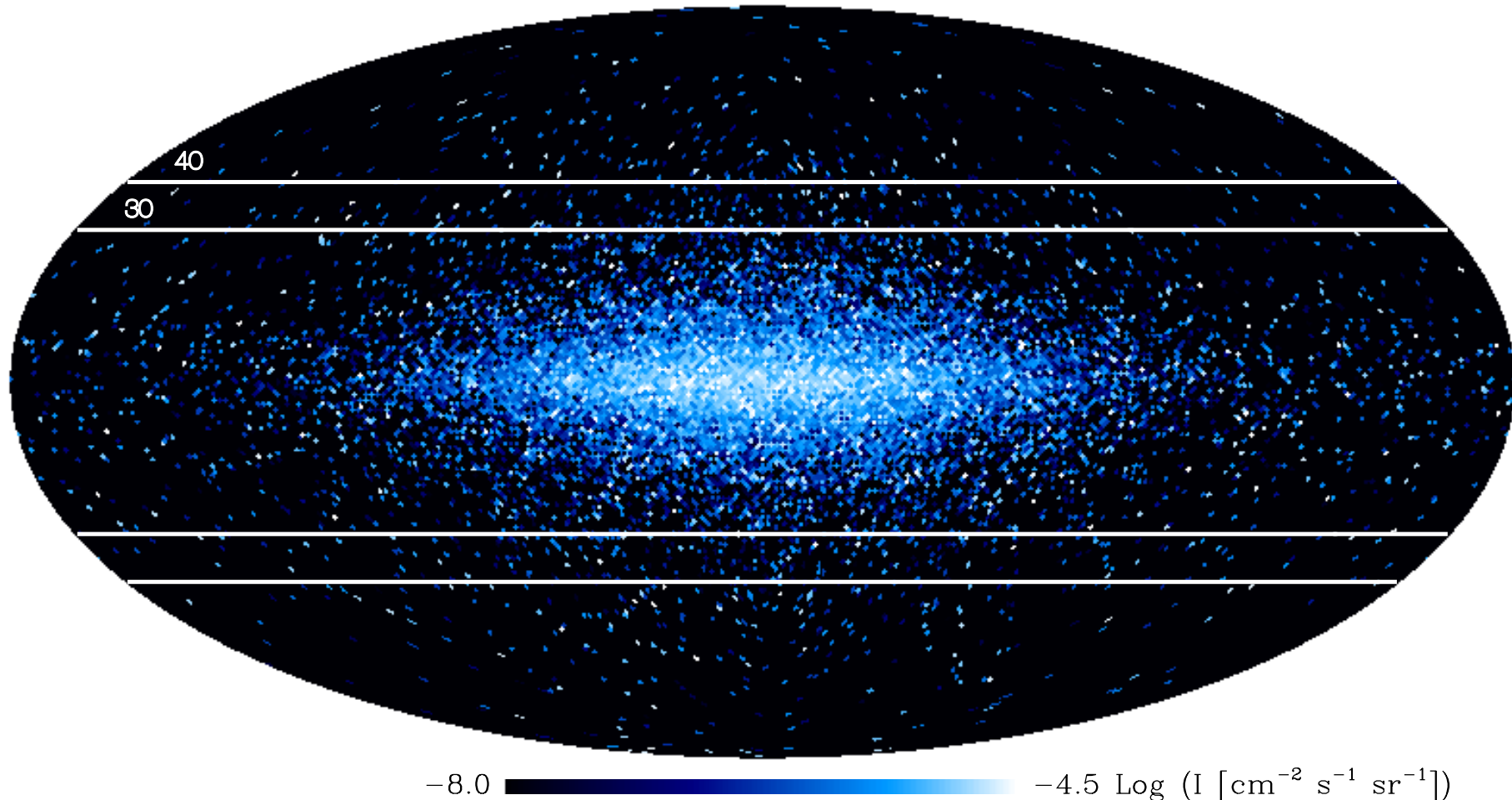
NB: these are indicative predicted values for source populations, taken from the literature.

- dependent on source model (large variations possible, especially for dark matter scenarios)
- dependent on source detection threshold
- for cosmological populations, dependent on EBL assumptions

These values may not be accurate for your favorite source population model.

IGRB anisotropies from millisecond pulsars

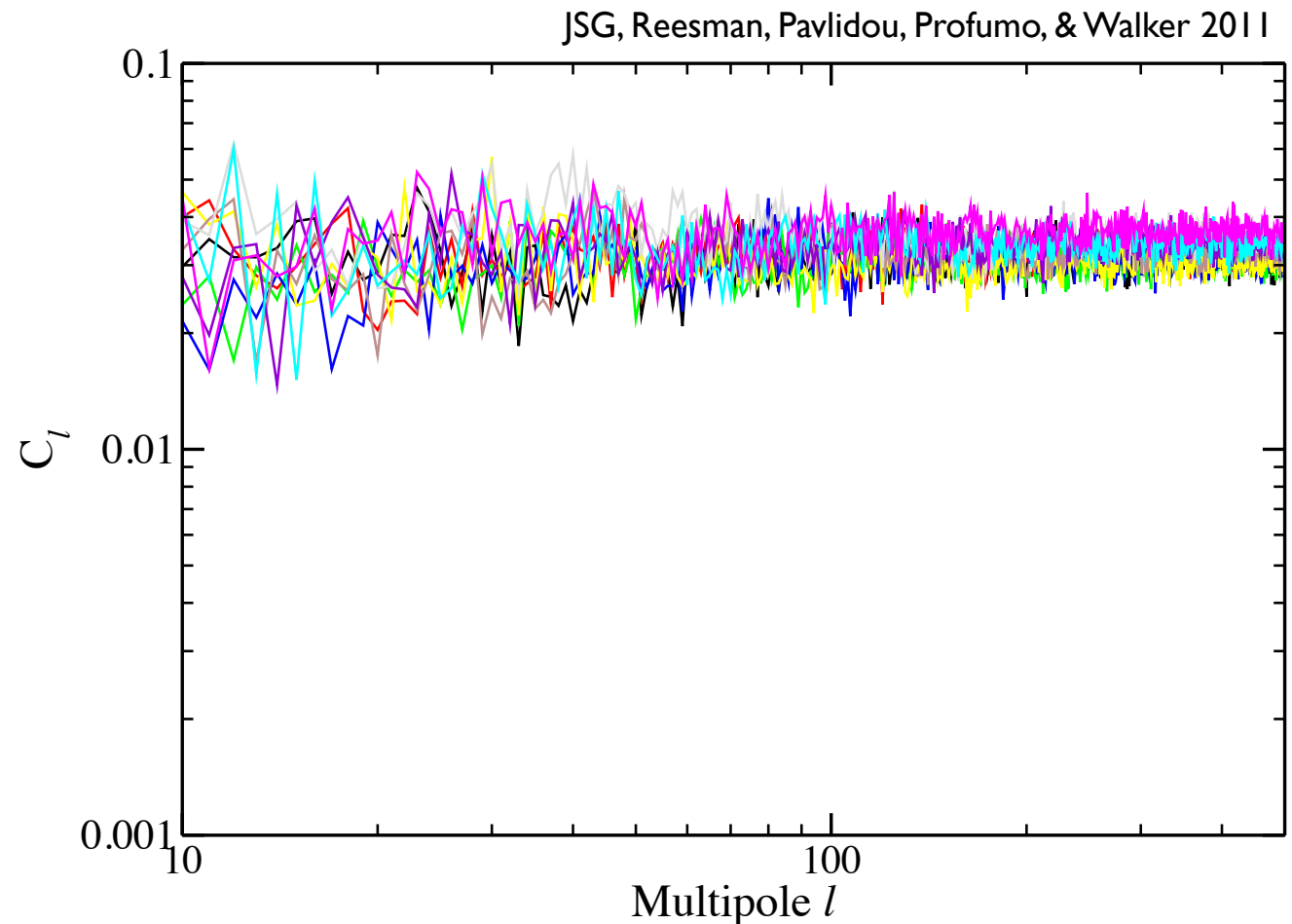
unresolved MSPs could contribute significantly to the high-latitude gamma-ray emission (e.g., Faucher-Giguere & Loeb 2009)



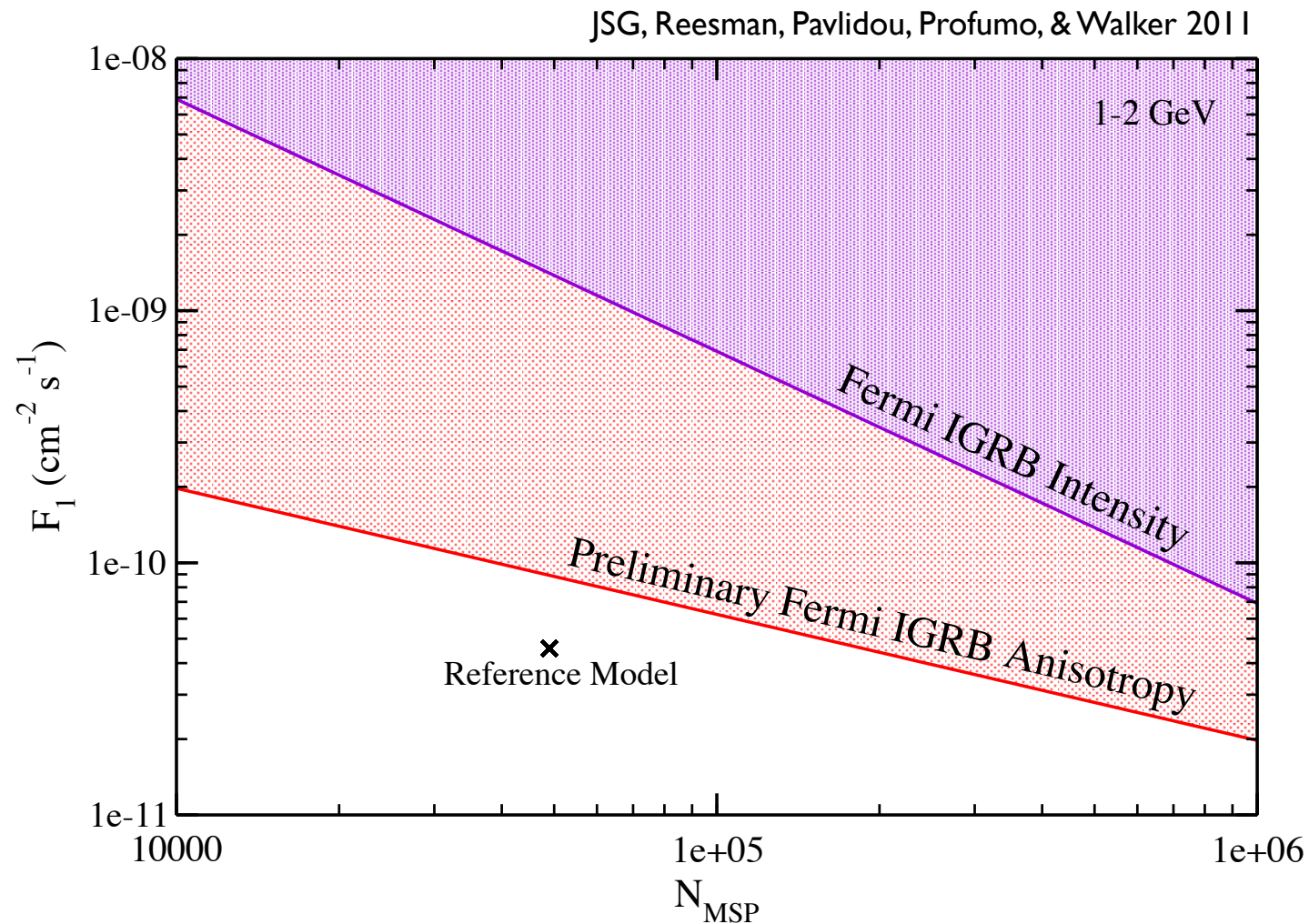
JSG, Reesman, Pavlidou, Profumo, & Walker 2011

Angular power spectrum of MSPs

- remarkably constant in multipole \rightarrow looks like emission from an unclustered source population (“Poisson-noise--like”)
- large amplitude anisotropy \rightarrow their diffuse contribution may be detectable/constrainable from Fermi data

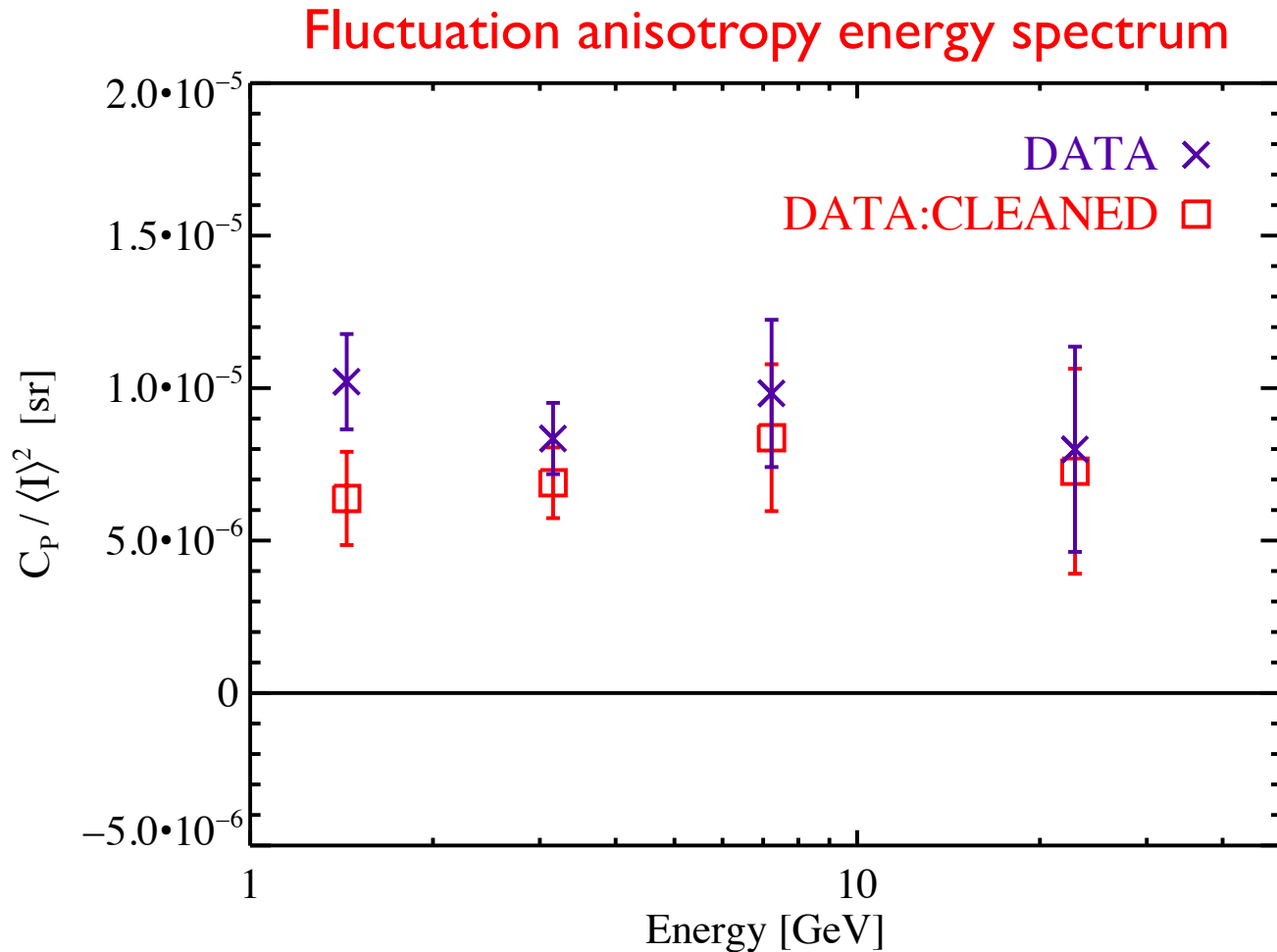


Constraints on the MSP population



- MSP models in shaded regions exceed measured IGRB intensity/anisotropy + 2-sigma
- anisotropy constraints ~ 1 order of magnitude stronger than intensity constraints

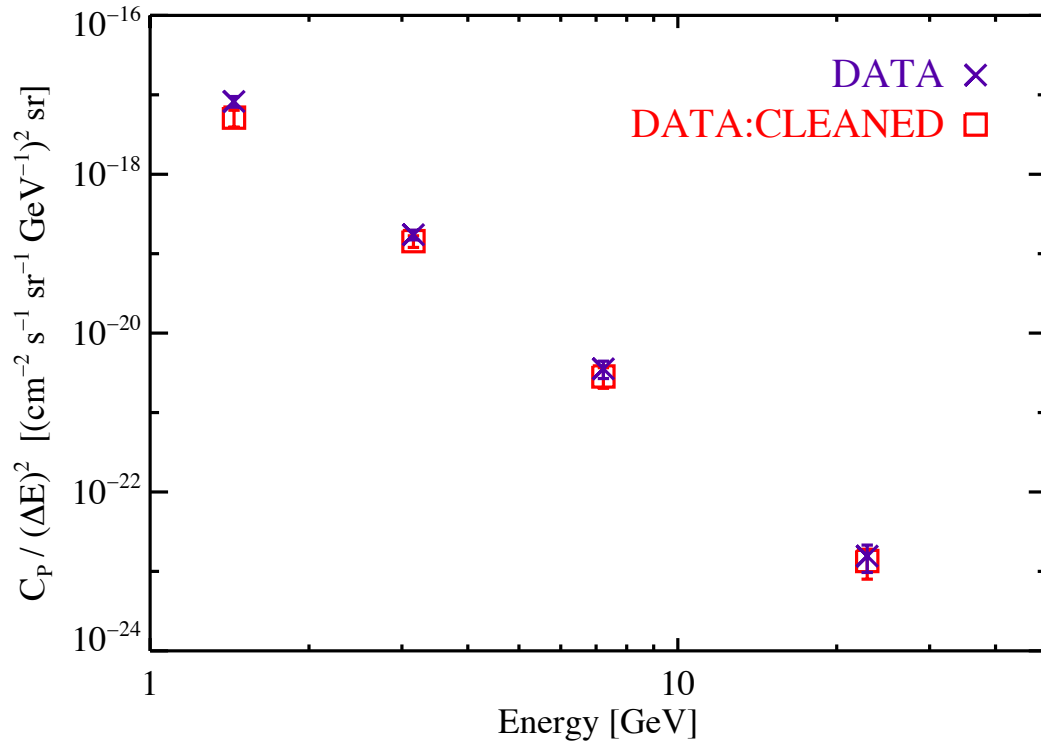
Energy dependence of anisotropy



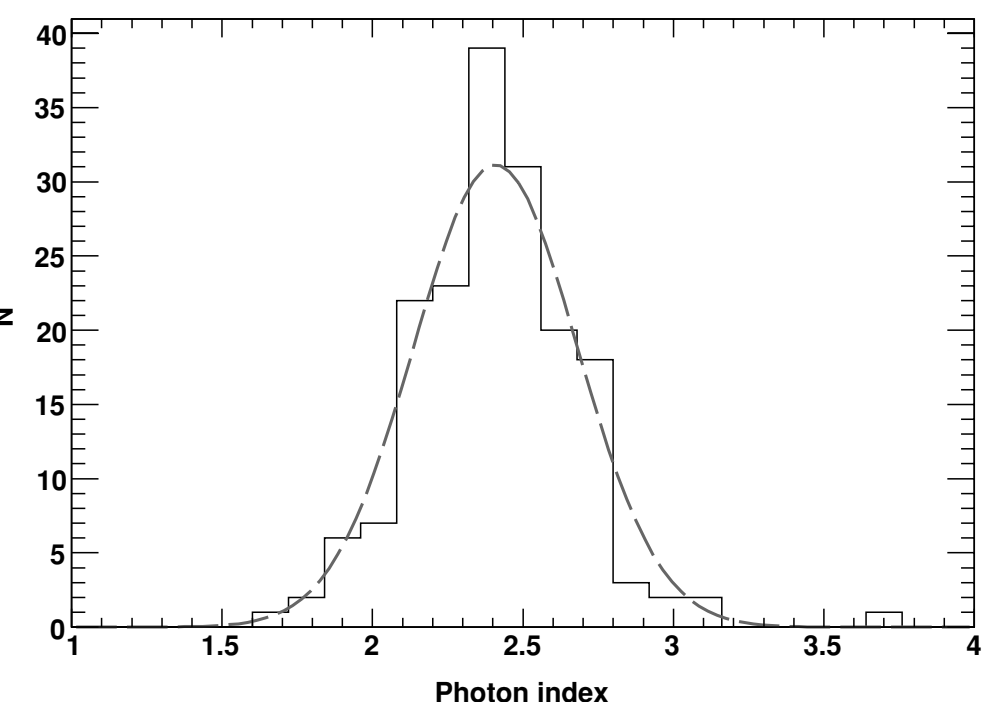
- consistent with no energy dependence, but mild or localized energy dependence not excluded
- consistent with all anisotropy contributed by one or more source classes contributing same fractional intensity at all energies considered

Energy dependence of anisotropy

Intensity anisotropy energy spectrum



Spectral indices of Fermi-LAT sources

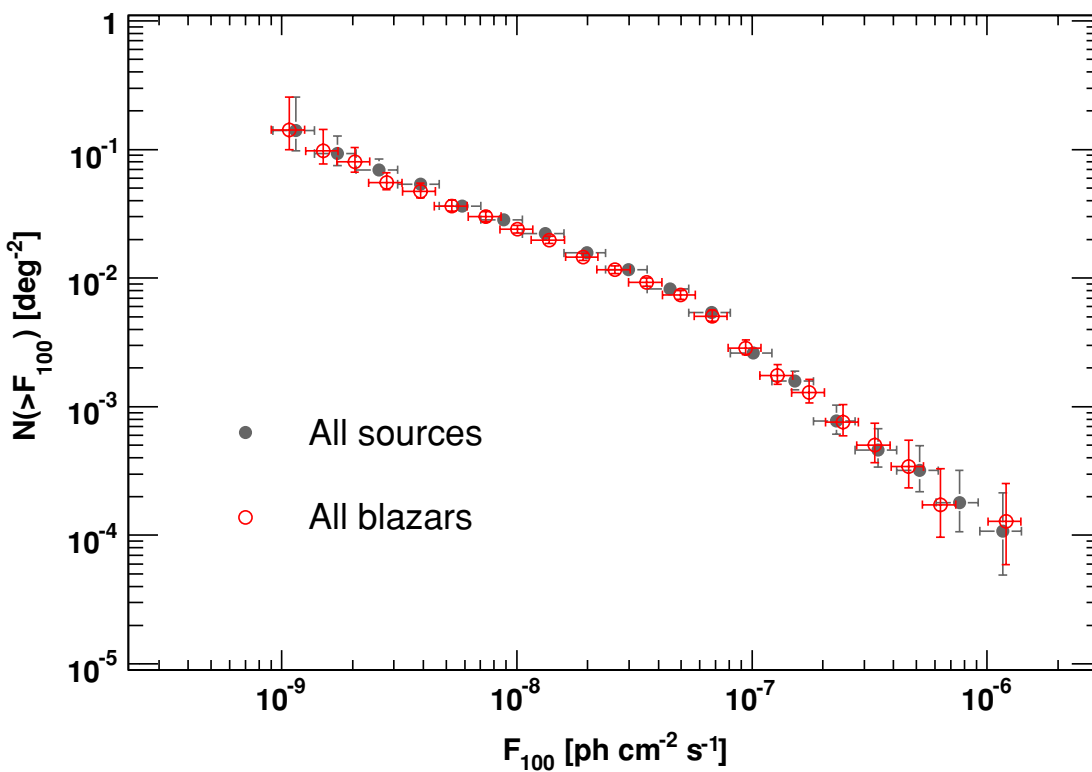


- consistent with that arising from a source class with power-law energy spectrum with $\Gamma = -2.40 \pm 0.07$ (-2.33 ± 0.08 for cleaned data)
- implied source spectral index is good agreement with mean intrinsic spectral index of blazars inferred from detected members

The source count distribution

the source count distribution (“LogN-LogS”) of Fermi-LAT–detected sources is consistent with a broken power law

LogN-LogS of Fermi LAT sources



Abdo et al. (Fermi LAT Collaboration), ApJ 720, 435 (2010)

high (bright-end)
spectral index

break flux

$\frac{dN}{dS} = \begin{cases} A S^{-\beta} & S \geq S_b \\ A S_b^{-\beta+\alpha} S^{-\alpha} & S < S_b \end{cases}$

low (faint-end)
spectral index

Anisotropy and source counts

the total intensity and Poisson angular power (C_P) from *unresolved* sources can be predicted from the source count distribution

$$I = \int_0^{S_t} \frac{dN}{dS} S dS \quad C_P = \int_0^{S_t} \frac{dN}{dS} S^2 dS$$

Anisotropy and source counts

the total intensity and Poisson angular power (C_P) from *unresolved* sources can be predicted from the source count distribution

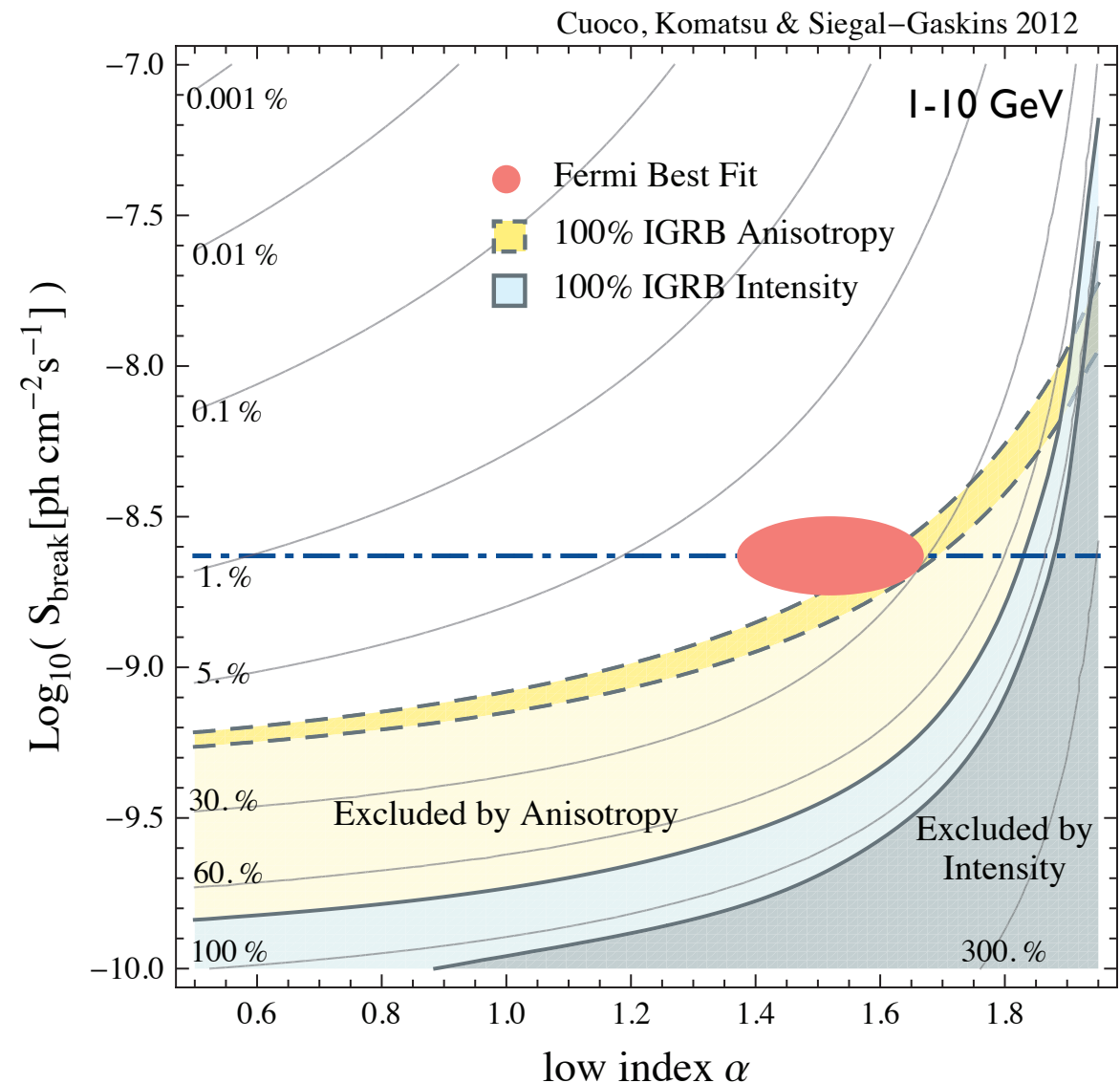
$$I = \int_0^{S_t} \frac{dN}{dS} S dS \quad C_P = \int_0^{S_t} \frac{dN}{dS} S^2 dS$$

How do the predicted intensity and angular power from unresolved blazars compare to the measured values?

Constraints on unresolved gamma-ray sources

- we fix the high index and normalization of the source count distribution to the measured best-fit values
- we vary the low index and break flux, and calculate the intensity and anisotropy produced by the unresolved sources in the 1-10 GeV band

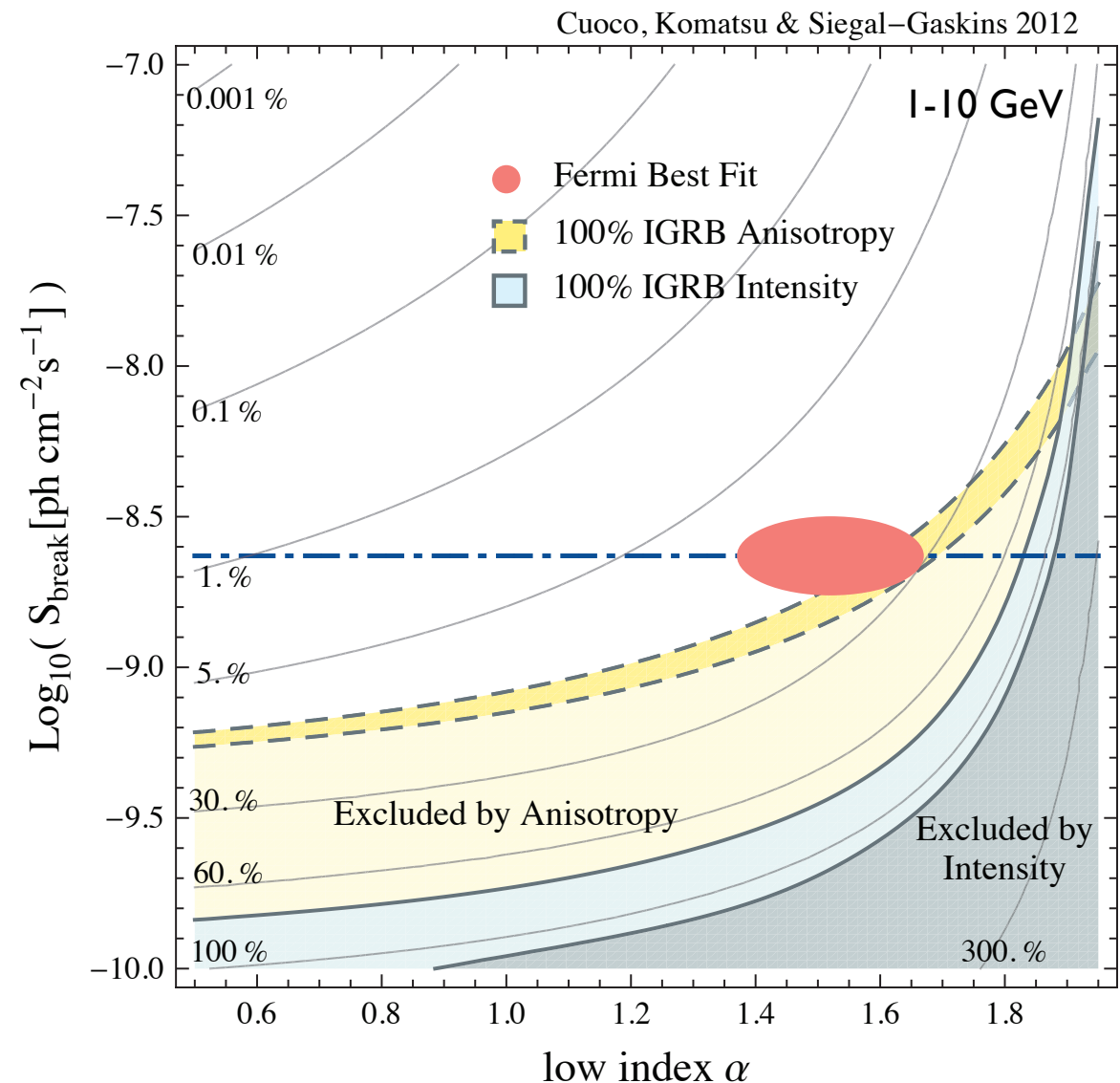
Constraints on source count distribution (logN-logS) parameter space



Constraints on unresolved gamma-ray sources

- we fix the high index and normalization of the source count distribution to the measured best-fit values
- we vary the low index and break flux, and calculate the intensity and anisotropy produced by the unresolved sources in the 1-10 GeV band
- anisotropy and source count analysis point to blazars contributing $\sim 30\%$ of IGRB intensity and $\sim 100\%$ of IGRB anisotropy

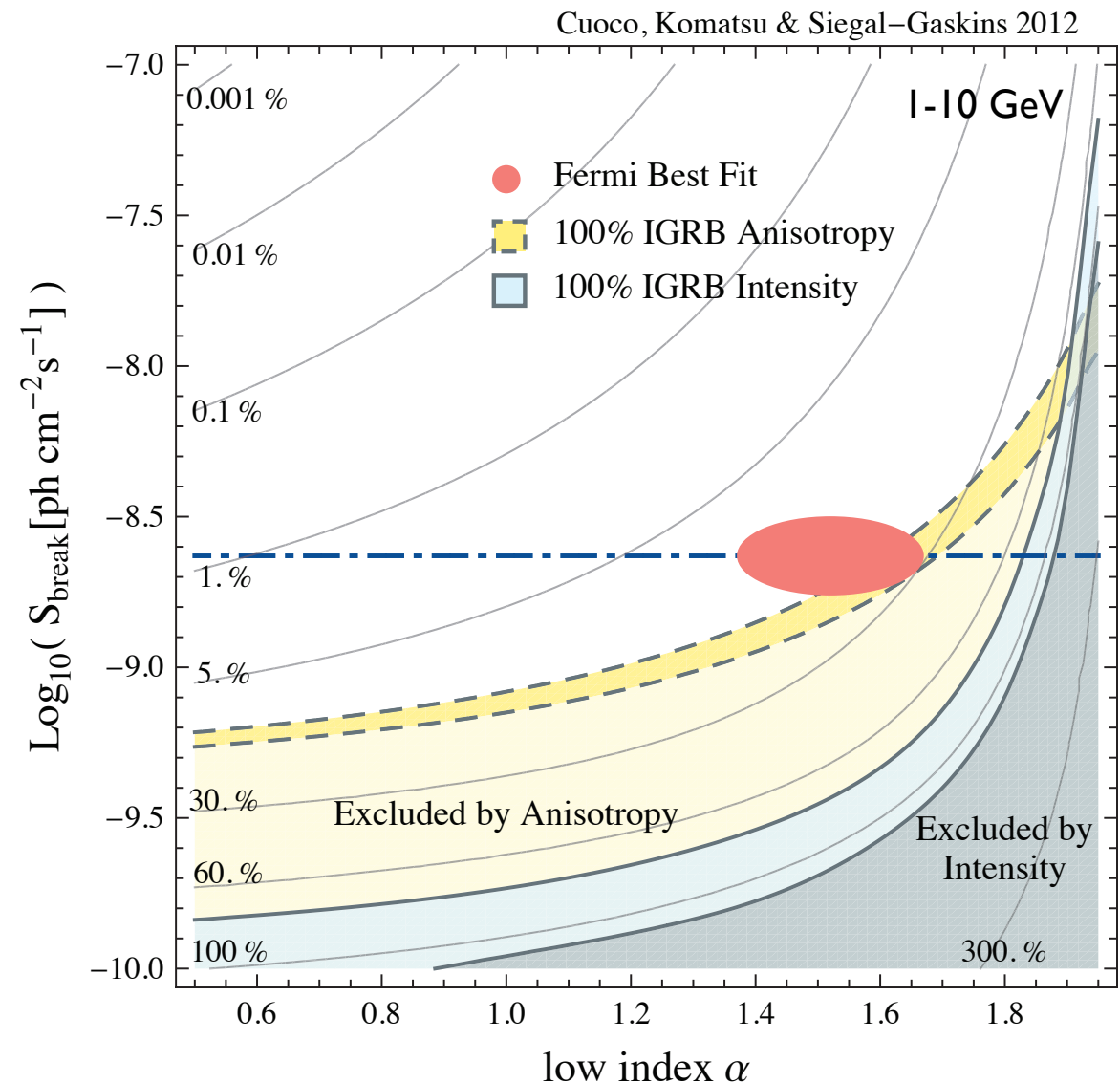
Constraints on source count distribution (logN-logS) parameter space



Constraints on unresolved gamma-ray sources

- we fix the high index and normalization of the source count distribution to the measured best-fit values
- we vary the low index and break flux, and calculate the intensity and anisotropy produced by the unresolved sources in the 1-10 GeV band
- anisotropy and source count analysis point to blazars contributing $\sim 30\%$ of IGRB intensity and $\sim 100\%$ of IGRB anisotropy
- this result implies that component(s) making $\sim 70\%$ of IGRB intensity have very low level of anisotropy

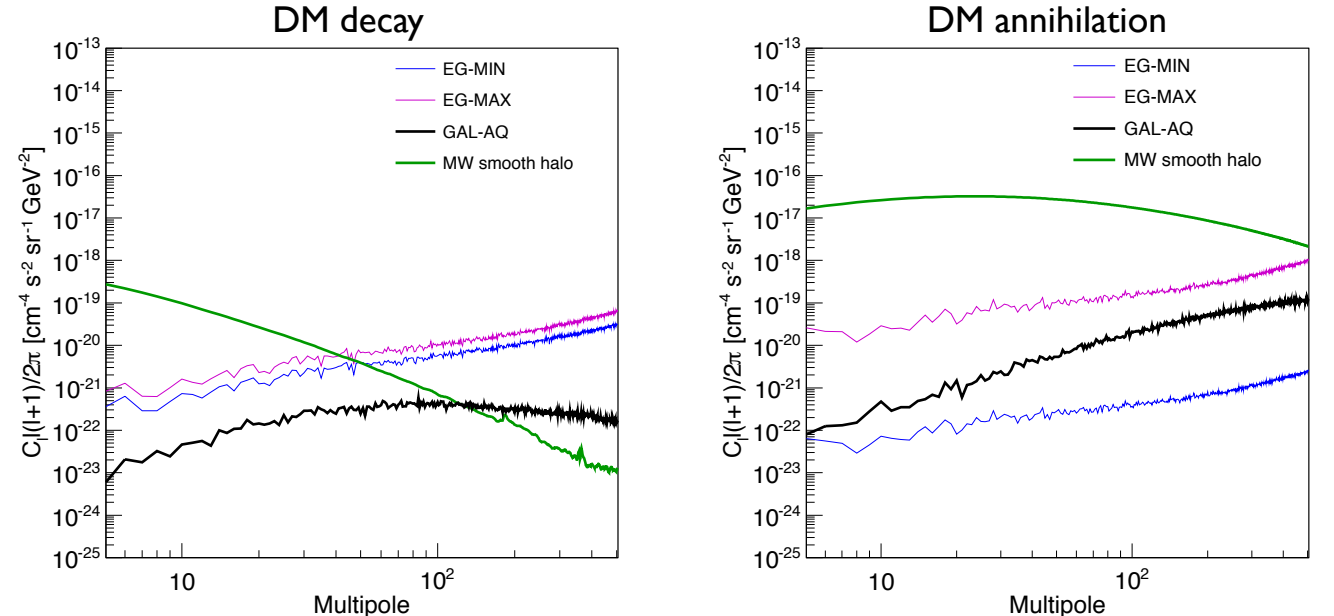
Constraints on source count distribution (logN-logS) parameter space



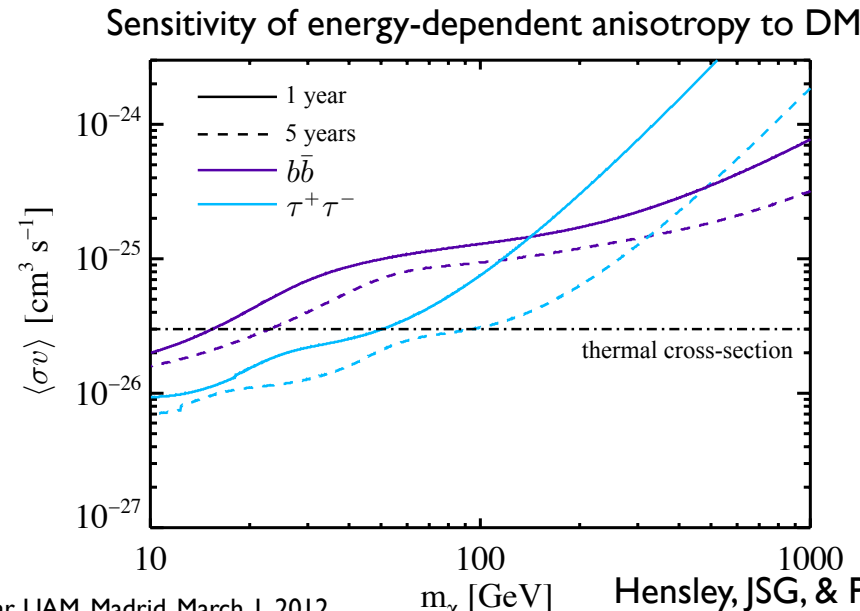
Dark matter implications

Joint project between Fermi LAT and MultiDark

- utilize high-resolution numerical simulations of the Galactic and extragalactic DM distribution (Aquarius and Millenium-II by the Virgo Consortium)
- predict the DM anisotropy signal from annihilation and decay, accurately accounting for redshifting and EBL attenuation for extragalactic DM, and secondary emission from Galactic DM
- extend and improve the Fermi LAT anisotropy measurement:
 - more data
 - improved data selections and instrument response
 - more energy bins and larger energy range
- compare the predicted angular power spectra to the measurement to place constraints on DM properties



Fornasa et al. 2012, in prep



Summary

- IGRB small-scale anisotropy has been detected for the first time!
- scale independence of high-multipole angular power suggests contribution from one or more unclustered point source populations
- measured angular power can be used to constrain the IGRB contribution from specific source classes
- lack of energy dependence of the fluctuation angular power suggests that the anisotropy is contributed primarily by one or more source populations with constant fractional contributions to the IGRB intensity over 1-50 GeV
- energy dependence of the intensity angular power is consistent with the anisotropy originating from a source population with a power-law energy spectrum with $\Gamma = -2.40 \pm 0.07$; this spectral index closely matches the inferred mean intrinsic spectral index of blazars
- source count analysis and anisotropy measurements point to blazars contributing $\sim 100\%$ of the anisotropy but only $\sim 30\%$ of the intensity of the IGRB

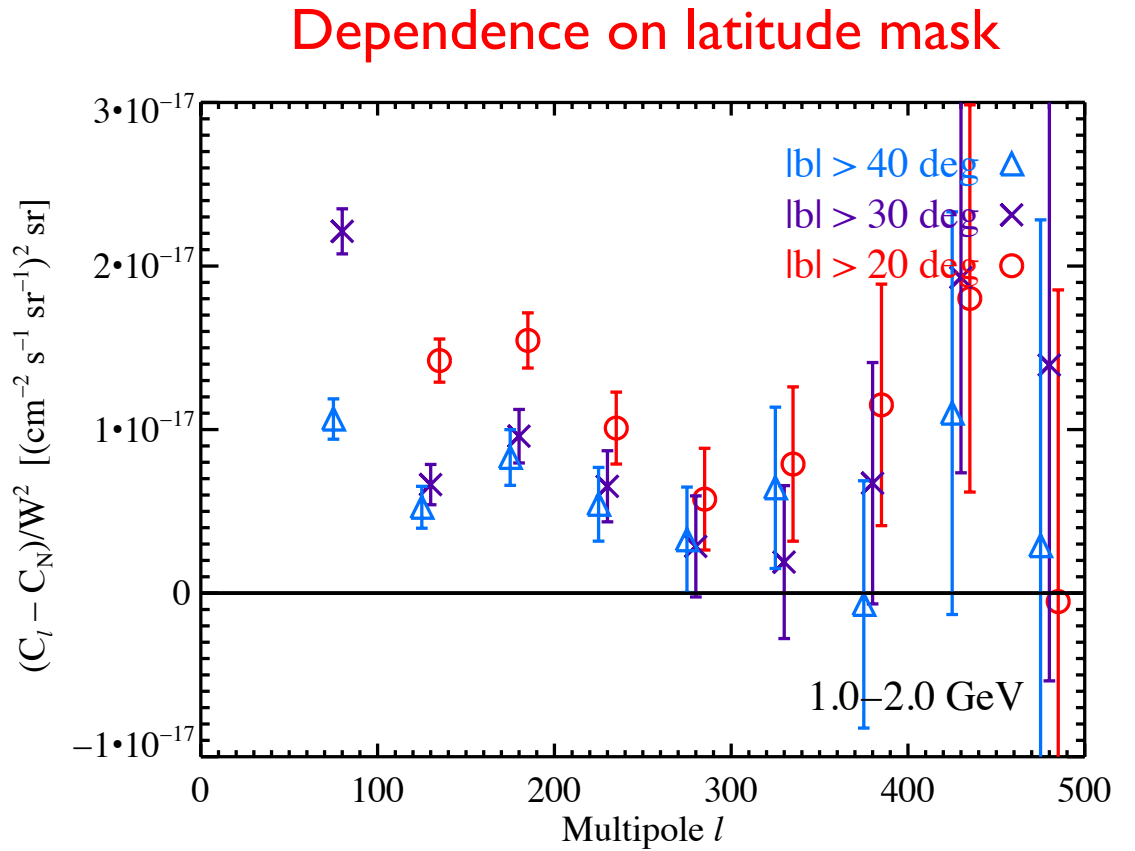
Additional slides

Analysis pipeline validation

- validation with a simulated source model: a source model with known anisotropy properties is simulated and analyzed using the same analysis pipeline as the data; the theoretically-predicted angular power spectrum is recovered
- dependence on the PSF model: no significant differences found between beam window functions for P6_V3 and P6_VII IRFs
- test for anisotropies induced by inaccuracies in the exposure map: an alternate exposure map is calculated directly from the data using an event-shuffling technique; angular power spectra are consistent with those using the exposure map from the Fermi Science Tools

Robustness to variations in masking

- dependence on the latitude mask: masking $|b| < 30$ deg is found to be sufficient to exclude significant contamination of the anisotropy above $l \sim 100$ by a component with a strong latitude dependence (e.g., Galactic diffuse emission)
- dependence on the source mask radius: no significant differences seen in multipole range of interest when mask angular radius is reduced from 2 deg to 1 deg

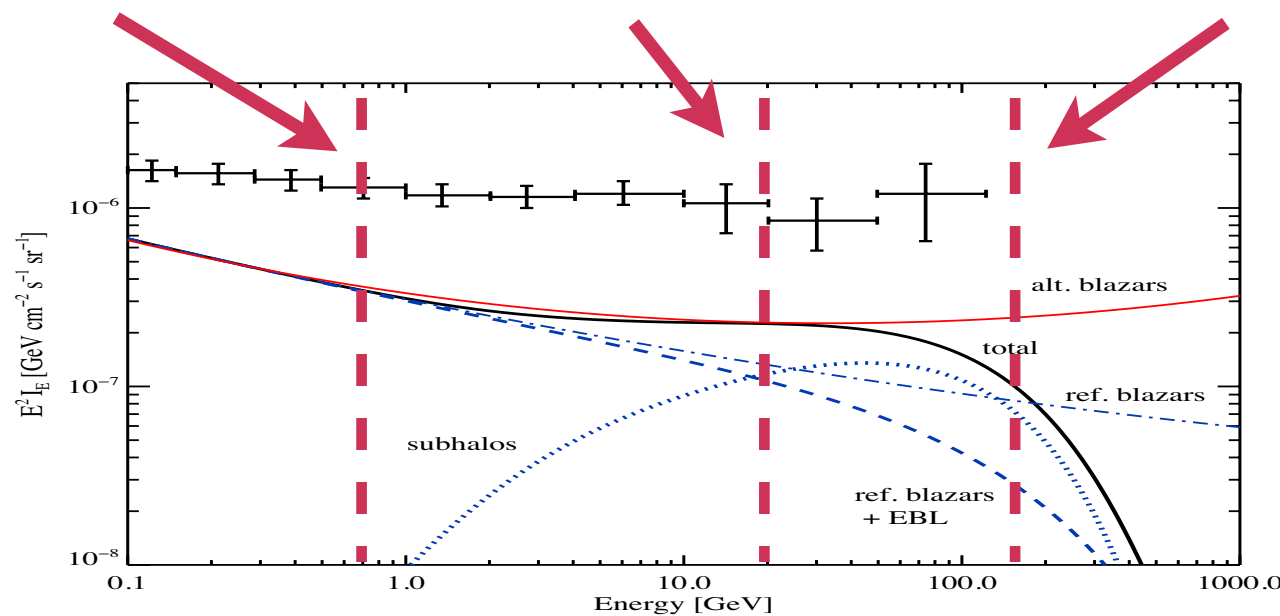
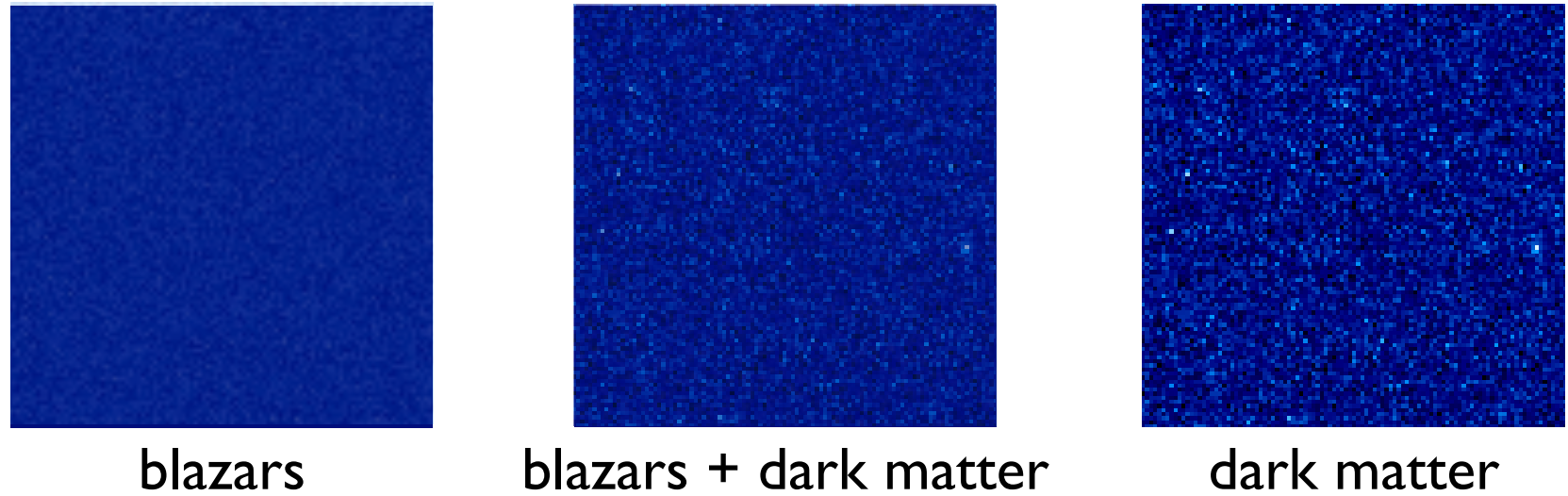


Exposure maps from an event-shuffling technique

- the exposure map is calculated directly from the data using an event-shuffling technique:
 - shuffling arrival times and arrival directions of real events *in instrument coordinates* generates a map indicating how an isotropic signal would appear in the LAT data
 - shuffled data map is directly proportional to the exposure map, with arbitrary normalization (hence only fluctuation angular power spectra can be calculated)
- data is analyzed as in default analysis, except shuffled map is used for the exposure
- provides a cross-check to ensure that the result is not biased by inaccuracies in the exposure calculation which could introduce spurious anisotropy signals

Energy-dependent anisotropy

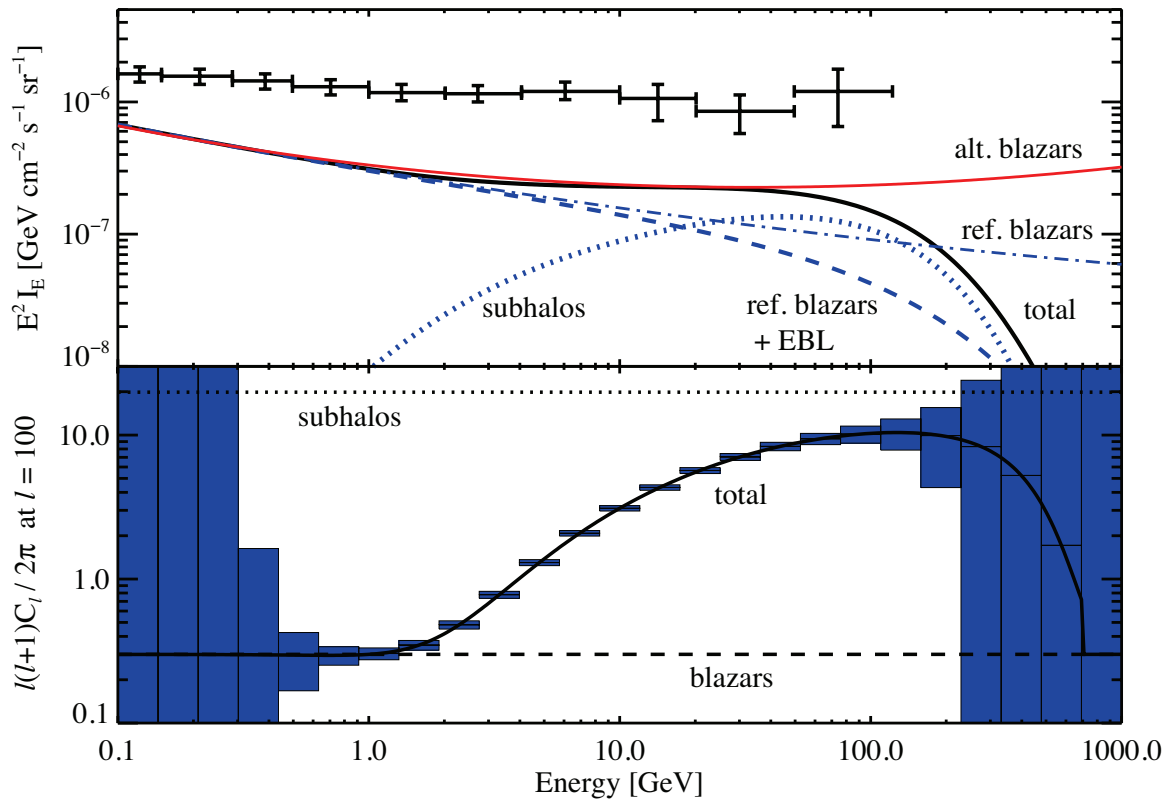
example patches of sky showing intensity fluctuations in units of the mean intensity



JSG & Pavlidou 2009

The anisotropy energy spectrum at work

neutralino mass = 700 GeV



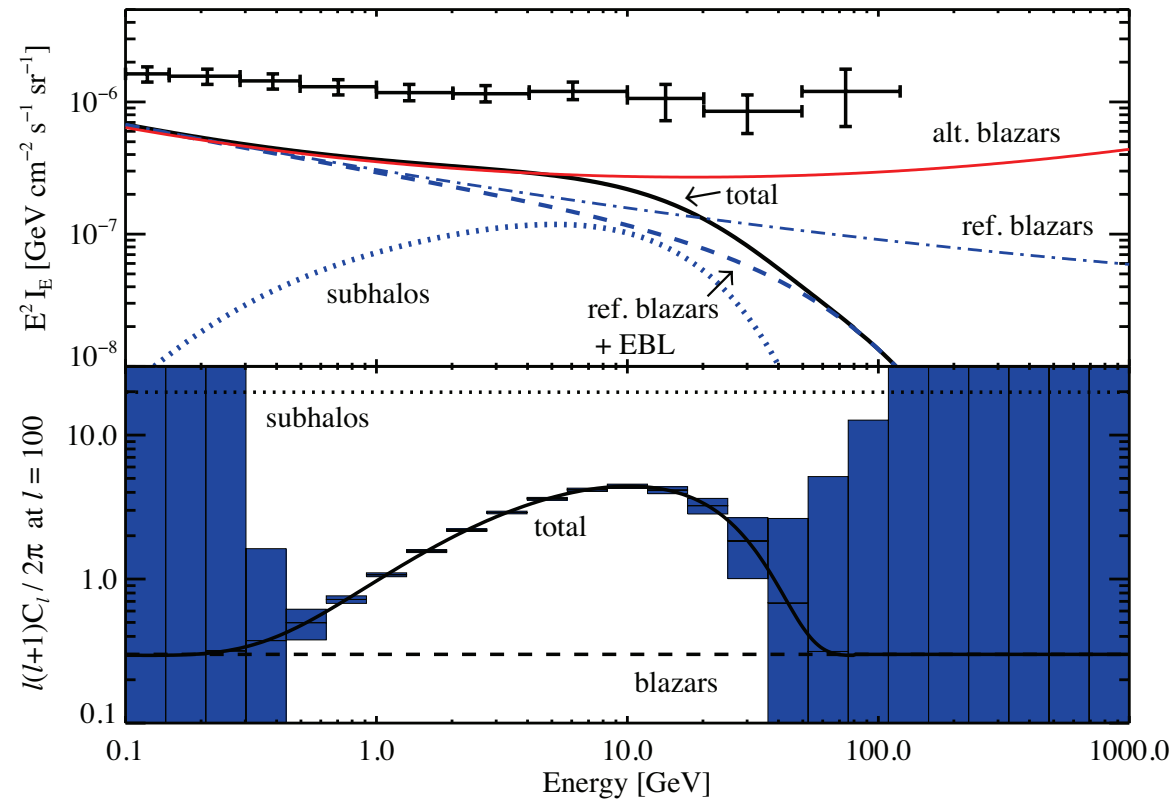
- 1-sigma errors
 - 5 years of Fermi all-sky observation
 - 75% of the sky usable
 - $N_b/N_s = 10 !!!!$
- error bars blow up at low energies due to angular resolution, at high energies due to lack of photons

JSG & Pavlidou 2009

- Galactic dark matter dominates the intensity above ~ 20 GeV, but spectral cut-off is consistent with EBL attenuation of blazars
- modulation of anisotropy energy spectrum is easily detected!

The anisotropy energy spectrum at work

neutralino mass = 80 GeV



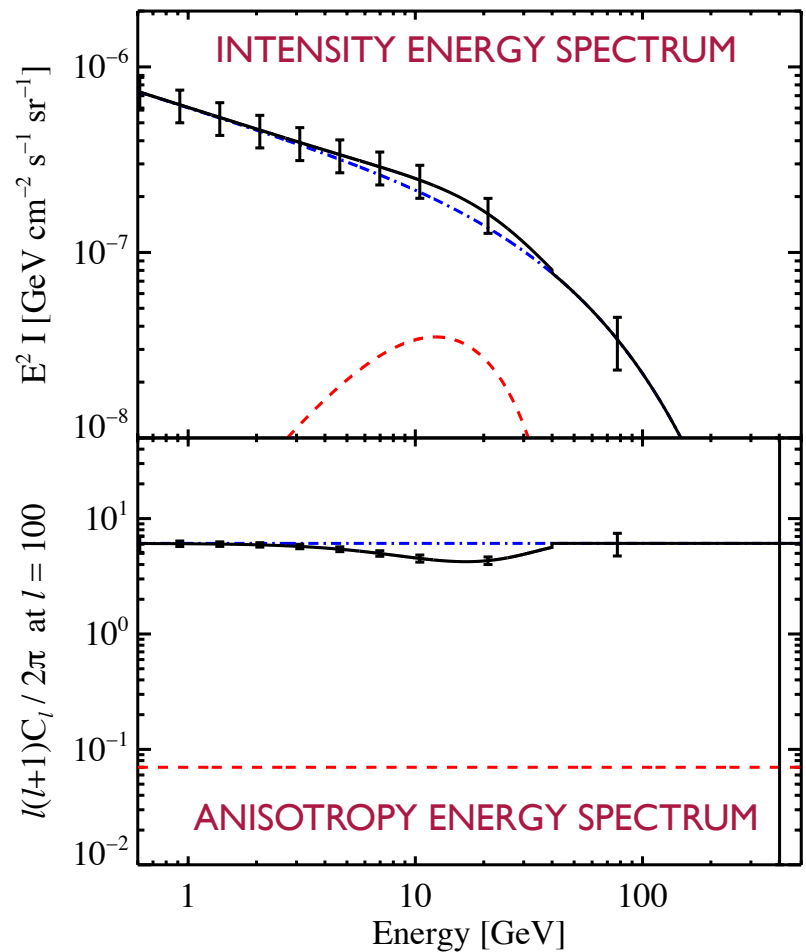
- 1-sigma errors
 - 5 years of Fermi all-sky observation
 - 75% of the sky usable
 - $N_b/N_s = 10 !!!!$
- error bars blow up at low energies due to angular resolution, at high energies due to lack of photons

- Galactic dark matter never dominates the intensity and spectral cut-off is consistent with EBL attenuation of blazars
- modulation of anisotropy energy spectrum is still strong!

A simple test to find multiple populations

- assume the large-scale isotropic diffuse (IGRB) is composed primarily of emission from blazars and dark matter
- fix the anisotropy properties of both populations, fix the blazar emission to a reference model, and vary the dark matter model parameters (mass, cross-section, annihilation channel)
- define a simple, ‘model-independent’ test criterion:
is the anisotropy energy spectrum at $E \geq 0.5$ GeV consistent with a constant value, equal to the weighted average of all energy bins?
- dark matter model is considered detectable if this hypothesis is rejected by a χ^2 test at 95% CL
- NB: this test is not optimized to find specific dark matter models; tailored likelihood analysis could significantly improve sensitivity!

example measurement
with 5 years of Fermi data

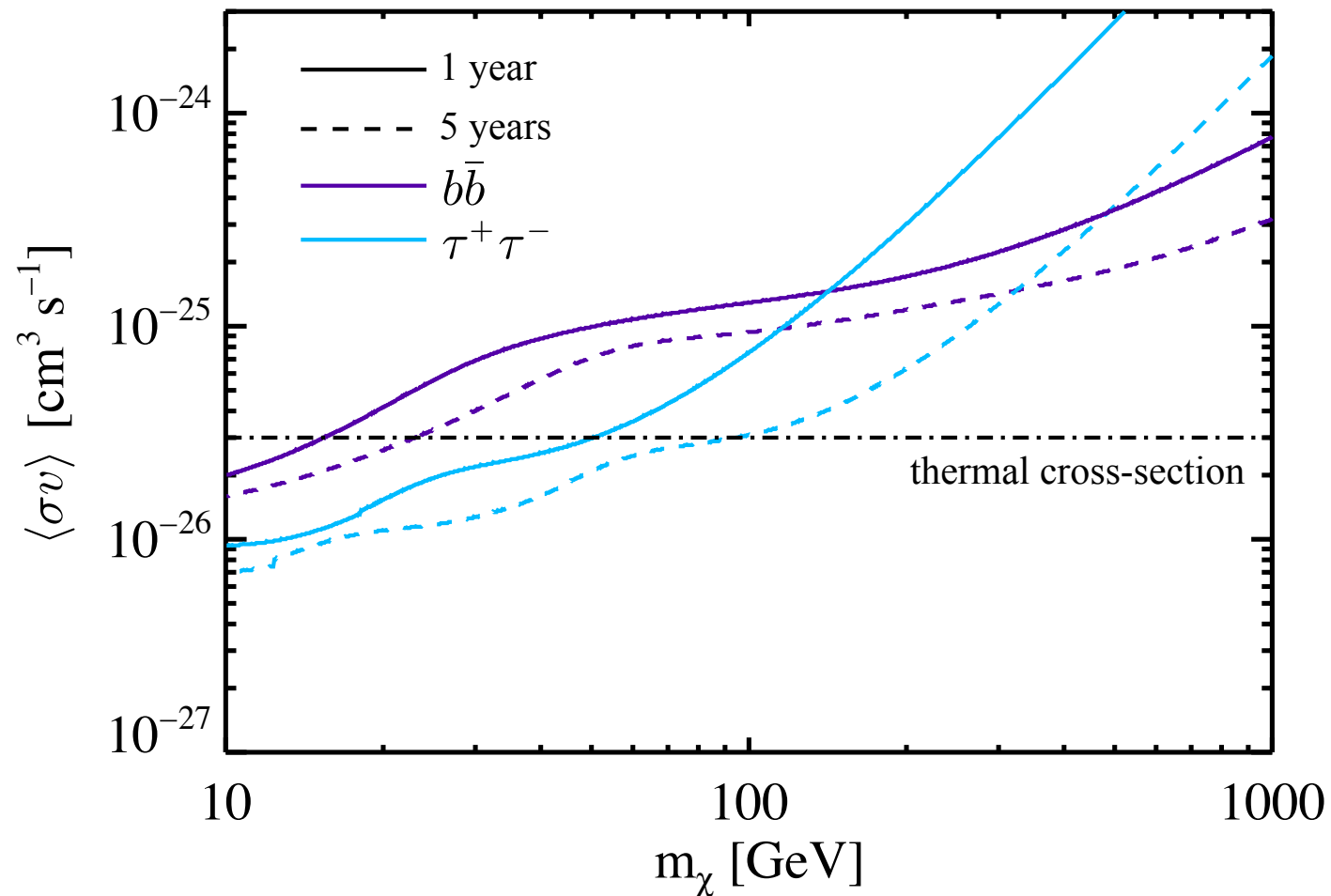


Hensley, JSG, & Pavlidou 2010

Sensitivity of the anisotropy energy spectrum

dark matter models above the curves are detectable by this test!

- DM produces a detectable feature in the anisotropy energy spectrum for a substantial region of parameter space in this scenario
- technique could probe cross-sections close to thermal; extends the reach of current indirect searches



Hensley, JSG, & Pavlidou 2010